doi:10.1038/nature21674

Supplemental Materials – Table of Contents

Section I: Archaeological Context and Sample Descriptions

A total of 55 samples were analysed within this study, including Neandertals (n=5), a great ape (n=1), monkeys (n=2), ancient Europeans (n=30), ancient Africans (n=8), and present-day humans (n= 9). The Australian Centre for Ancient DNA (ACAD) and museum collection sample numbers, sample information, dating results, and classifications based on culture, group and period are given in Table S1. Samples were classified according to both geographic and cultural information (Culture or Group; Table S1) or chronographic information (Period; Table S1). The archaeological context of several European dental calculus samples and their cultures (*i.e.* Jewbury, Raunds, St. Helen on Walls, Bronze Age, and LBK Halberstadt) have been described previously by Adler *et al*[1]. Similarly, the context for new samples from a Linear Band Pottery culture (LBK) site near Stuttgart-Muhlhausen, Germany has also been previously described[2]. In addition, modern samples from healthy, 22-40 year old male and female volunteers at the University of Adelaide, Australia were included from a previous study[1]. The archaeological and anthropological context surrounding the remaining ancient and historic dental calculus samples is described within the following section.

Table S1 – Sample names, descriptions, and archaeological information associated with each sample used within this study is listed. If calculus samples were analyzed in a previous study, the reference is given. The data type obtained from each samples is also noted.

ACAD Number	Description	Figure Abbreviations	Host Species	Culture or Group	Archaeological Site Location	Museum Sample Number	Museum	Date(yBP)	16S or Shotgun Sequencing	Calculus Sample Reference
12055	Neandertal – Spy I	Spy I	*Homo neandertalensis*	Paleolithic	Spy Cave, Belgium	Spy II (94a)	Royal Belgian Institute of Natural Sciences, Brussels, Belgium	35,810+260	16S/Shotgun	(this study)
14017	Neandertal – Spy II	Spy II	*Homo neandertalensis*	Paleolithic	Spy Cave, Belgium	Spy I (92b)	Royal Belgian Institute of Natural Sciences, Brussels, Belgium	36,350+310	16S/Shotgun	(this study)
12056	Neandertal - El Sidrón1	ElSidron1	*Homo neandertalensis*	Paleolithic	El Sidrón Cave, Spain	El Sidrón 1 SD 1427C	Museo Nacional de Ciencias Naturales, Madrid	~49,000yBP	16S/Shotgun	(this study)
12057	Neandertal - El Sidrón2	ElSidron2	*Homo neandertalensis*	Paleolithic	El Sidrón Cave, Spain	El Sidrón 6 SD 1604	Museo Nacional de Ciencias Naturales, Madrid	~49,000yBP	16S/Shotgun	(this study)
8911	Neandertal - Bruel Grotta	N/A	*Homo neandertalensis*	Paleolithic	Bruel Grotta, Italy	8911	University of Florence, Italy	nd	nd	(this study)
12014	Mesolithic - Poland 1	EuroHG1	*Homo sapiens*	Hunter-gatherer	Dudka, Poland	nd	University of Warsaw, Poland	~7550	16S/Shotgun	14
12017	Mesolithic - Poland 2	EuroHG2	*Homo sapiens*	Hunter-gatherer	Dudka, Poland	VI-7 A	University of Warsaw, Poland	~7550	16S/Shotgun	14
12826	LBK - Stuttgart, Germany 1	LBK1	*Homo sapiens*	Neolithic	Stuttgart-Mühlhausen I, Germany	762	Landesdenkmalpflege Baden-Württemberg, University of Tübingen, Germany	~7440	16S/Shotgun	(this study)
12829	LBK - Stuttgart, Germany 2	LBK2	*Homo sapiens*	Neolithic	Stuttgart-Mühlhausen I, Germany	765	Landesdenkmalpflege Baden-Württemberg, University of Tübingen, Germany	~7440	16S/Shotgun	(this study)
12824	LBK - Stuttgart, Germany 3	LBK3	*Homo sapiens*	Neolithic	Stuttgart-Mühlhausen I, Germany	760	Landesdenkmalpflege Baden-Württemberg, University of Tübingen, Germany	~7440	16S/Shotgun	(this study)
12830	LBK - Stuttgart, Germany 4	LBK4	*Homo sapiens*	Neolithic	Stuttgart-Mühlhausen I, Germany	766	Landesdenkmalpflege Baden-Württemberg, University of Tübingen, Germany	~7440	16S	(this study)
8240	LBK - Halberstadt, Germany 1	LBKH1	*Homo sapiens*	Neolithic	LBK - Halberstadt-Sonntagsfeld 1	HAL25b	Landesmuseum Sachsen-Anhalt, Germany	~7440	16S	14
8277	LBK - Halberstadt, Germany 2	LBKH2	*Homo sapiens*	Neolithic	LBK - Halberstadt-Sonntagsfeld 2	HAL39a	Landesmuseum Sachsen-Anhalt, Germany	~7440	16S	14
11105	Early Neolithic - Sudan 1	AfrSud1	*Homo sapiens*	African Early Neolithic	Al Khiday, Sudan	16D4 grave93	Durham University, England	~5,000yBP	16S/Shotgun	(this study)
11106	Early Neolithic - Sudan 2	AfrSud2	*Homo sapiens*	African Early Neolithic	Al Khiday, Sudan	16D4 grave96	Durham University, England	~5,000yBP	16S/Shotgun	(this study)
4331	BellBeaker - Germany	BB	*Homo sapiens*	Bell Beaker	BellBeaker - Quedlinburg XII	Befund 967	Landesmuseum Sachsen-Anhalt, Germany	~4450	16S	14
9436	LNBA - Germany	LNBA	*Homo sapiens*	Late Neolithic, Bell Beaker	LNBA - Benzingerode-Heimburg	BZH17	Landesmuseum Sachsen-Anhalt, Germany	~4150	16S	14
8890	Bronze Age - England 1	BA1	*Homo sapiens*	Bronze Age	Yorkshire, England	T82GF	University of Aberdeen, Scotland	~4150	16S	14
8891	Bronze Age - England 2	BA2	*Homo sapiens*	Bronze Age	Yorkshire, England	14Barrow163	University of Aberdeen, Scotland	~4150	16S	14
13207	Pre-pastoralist Period - South Africa 2	AfrSF1	*Homo sapiens*	African LSA	Near Cape Town, South Africa	UCT 169	Department of Human Biology of the University of Cape Town, South Africa	2320+/-50yrsBP	16S/Shotgun	(this study)
13208	Pre-pastoralist Period - South Africa 3	AfrSF2	*Homo sapiens*	African LSA	Near Cape Town, South Africa	UCT 373	Department of Human Biology of the University of Cape Town, South Africa	3835+/-50yrsBP	16S/Shotgun	(this study)
13209	Pre-pastoralist Period - South Africa 4	AfrSF3	*Homo sapiens*	African LSA	Near Cape Town, South Africa	UCT 386	Department of Human Biology of the University of Cape Town, South Africa	2000+/-50yrsBP	16S	(this study)
13210	Pre-pastoralist Period - South Africa 5	AfrSF4	*Homo sapiens*	African LSA	Near Cape Town, South Africa	UCT 421	Department of Human Biology of the University of Cape Town, South Africa	2895+/-45BP	16S	(this study)
13211	Pre-pastoralist Period - South Africa 6	AfrSF5	*Homo sapiens*	African LSA	Near Cape Town, South Africa	UCT 427	Department of Human Biology of the University of Cape Town, South Africa	2670+/-80yrsBP	16S	(this study)
Warinner_B61	Medieval - Germany	War_B61	*Homo sapiens*	Dalheim	Dalheim, Germany	B61	University of Zürich's Institute of Anatomy, Switzerland	c.950–1200CE	Shotgun	15
Warinner_G12	Medieval - Germany	War_G12	*Homo sapiens*	Dalheim	Dalheim, Germany	G12	University of Zürich's Institute of Anatomy, Switzerland	c.950–1200CE	Shotgun	15
8333	Early Rural Medieval - England 1	RM1	*Homo sapiens*	Raunds Furnells	Northamptonshire, England	R5287	University of Aberdeen, Scotland	~1100	16S	14
8335	Early Rural Medieval - England 2	RM2	*Homo sapiens*	Raunds Furnells	Northamptonshire, England	R5252	University of Aberdeen, Scotland	~1100	16S	14
8336	Early Rural Medieval - England 3	RM3	*Homo sapiens*	Raunds Furnells	Northamptonshire, England	R5008	University of Aberdeen, Scotland	~1100	16S	14
8869	Early Rural Medieval - England 4	RM4	*Homo sapiens*	Raunds Furnells	Northamptonshire, England	R5229	University of Aberdeen, Scotland	~1100	16S	14
8874	Late Rural Medieval - St Helens, England 11	RMS1	*Homo sapiens*	St. Helens on the Walls	York, England	5241	University of Aberdeen, Scotland	~1100	16S	14
8330	Late Urban Medieval - England 1	Jewbury1	*Homo sapiens*	Jewbury	York, England	J2303	Jewbury Cemetery, England	~750	16S	14
8332	Late Urban Medieval - England 2	Jewbury2	*Homo sapiens*	Jewbury	York, England	J1336	Jewbury Cemetery, England	~750	16S	14
8477	Late Urban Medieval - England 3	UM3	*Homo sapiens*	Jewbury	York, England	2357	Jewbury Cemetery, England	~750	16S	14
8482	Late Urban Medieval - England 5	UM4	*Homo sapiens*	Jewbury	York, England	2358	Jewbury Cemetery, England	~750	16S	14
8812	Late Urban Medieval - England 1 (QG)	UM5	*Homo sapiens*	Jewbury	York, England	J2360	Jewbury Cemetery, England	~750	16S/Shotgun	(this study)
8824	Late Urban Medieval - England 2 (QG)	UM6	*Homo sapiens*	Jewbury	York, England	J2454	Jewbury Cemetery, England	~750	16S/Shotgun	(this study)
13213	Pastoralist Period - South Africa 1	AfrPP1	*Homo sapiens*	African Pastoralist Period	Near Cape Town, South African	UCT 582	Department of Human Biology of the University of Cape Town, South Africa	740+/-40yrsBP	16S/Shotgun	(this study)
13204	Pastoralist Period - South Africa 2	AfrPP2	*Homo sapiens*	African Pastoralist Period	Near Cape Town, South African	UCT 67	Department of Human Biology of the University of Cape Town, South Africa	570+/-45yrsBP	16S/Shotgun	(this study)
13206	Pastoralist Period - South Africa 3	AfrPP3	*Homo sapiens*	African Pastoralist Period	Near Cape Town, South African	UCT 157	Department of Human Biology of the University of Cape Town, South Africa	587+/-28yrsBP	16S	(this study)
13227	Post-Industrial Revolution - Germany 1	IndRev1	*Homo sapiens*	Post-Industrial Revolution	Hettstedt Gymnasium, Germany	23	Johannes Gutenberg University, Mainz, Germany	1860-1865	16S/Shotgun	(this study)
13230	Post-Industrial Revolution - Germany 2	IndRev2	*Homo sapiens*	Post-Industrial Revolution	Hettstedt Gymnasium, Germany	43	Johannes Gutenberg University, Mainz, Germany	1860-1865	16S/Shotgun	(this study)
13232	Post-Industrial Revolution - Germany 3	IndRev3	*Homo sapiens*	Post-Industrial Revolution	Hettstedt Gymnasium, Germany	85	Johannes Gutenberg University, Mainz, Germany	1860-1865	16S	(this study)
P2	Modern Plaque 2	ModernP2	*Homo sapiens*	Modern Plaque	Adelaide, Australia	P2	University of Adelaide Dental School, Australia	0	16S	14
P6	Modern Plaque 6	ModernP6	*Homo sapiens*	Modern Plaque	Adelaide, Australia	P6	University of Adelaide Dental School, Australia	0	16S	14
P7	Modern Plaque 7	ModernP7	*Homo sapiens*	Modern Plaque	Adelaide, Australia	P7	University of Adelaide Dental School, Australia	0	16S	14
P8	Modern Plaque 8	ModernP8	*Homo sapiens*	Modern Plaque	Adelaide, Australia	P8	University of Adelaide Dental School, Australia	0	16S	14
P10	Modern Plaque 10	ModernP10	*Homo sapiens*	Modern Plaque	Adelaide, Australia	P10	University of Adelaide Dental School, Australia	0	16S	14
C5	Modern Calculus 5	ModernC5	*Homo sapiens*	Modern Calculus	Adelaide, Australia	C5	University of Adelaide Dental School, Australia	0	16S	14
C8	Modern Calculus 6	ModernC8	*Homo sapiens*	Modern Calculus	Adelaide, Australia	C8	University of Adelaide Dental School, Australia	0	16S	14
C7	Modern Calculus 7	ModernC7	*Homo sapiens*	Modern Calculus	Adelaide, Australia	C7	University of Adelaide Dental School, Australia	0	16S	14
C10	Modern Calculus 10	Modern	*Homo sapiens*	Modern Calculus	Adelaide, Australia	C10	University of Adelaide Dental School, Australia	0	16S/Shotgun	14
12873	Chimpanzee	Chimp	*Pan troglodytes*	Primate, wild caught	Gola Forest, Sierra Leone	810	Odontological Collection, The Royal College of Surgeons, England	~70yBP	16S/Shotgun	(this study)
12878	Macaque	N/A	*Macaca mulatta*	Primate, captive	nd	814	Odontological Collection, The Royal College of Surgeons, England	nd	16S	(this study)
12887	Baboon	N/A	*Papio anubis*	Primate, captive	nd	815	Odontological Collection, The Royal College of Surgeons, England	nd	16S	(this study)
8483	Tooth - England	N/A	Environmental	Tooth	York, England	2665	Jewbury Cemetery, England	~750	16S	14

Neandertals

The Neandertal dental calculus examined within this study was accessed from several different collections: Royal Belgian Institute of Natural Sciences in Brussels, Belgium, the Museo Nacional de Ciencias Naturales, in Madrid, Spain, and University of Florence in Florence, Italy.

The two Neandertal specimens from Spy cave, Belgium were obtained from separate Neandertal specimens, Spy I and Spy II, from the Royal Belgian Institute of Natural Sciences in Brussels, Belgium, and were dated in 2009 to be ~36,000 yBP[3]. The Spy I supra-gingival calculus sample was collected from the lower M3 (Spy 94a), while the Spy II supra-gingival calculus sample was obtained from the lower M2 (92b). Although both individuals had calculus, their general oral health was excellent, with no cavities, abscesses, or major signs of periodontal disease. Spy I possesses tooth picking grooves on the upper and lower premolars and molars, while Spy II does not display any traces of tooth picking. This could be related to individual behaviour or to differential periodontal health. No DNA studies resolving the sex of these two specimens have been published, but skeletal evidence suggests that there is one male and one female specimen.

The dental calculus sample from El Sidrón 1 (1427c) was supra-gingival calculus from the lower molar of adult 2 (a young male, as determined by genetics and morphology of the mandible), whereas the calculus sample from El Sidrón 2 (1604) corresponds to adult 4 (female, as determined by skeletal morphology and canines)[4]. These two individuals have different mitochondrial lineages[4]. Although these two individuals are not maternally related, geological, archaeological, and genetic evidence has revealed that the El Sidrón individuals correspond to a contemporaneous social group of Neandertals, rapidly accumulated in the side gallery

of a phreatic cave system through a collapse infill process. Analysis of the dentition in the young adult Neandertal male (El Sidrón 1) suggests he may have suffered from oral disease, as demonstrated by large calculus deposits and the presence of an abscess in the lower jaw[4]. Recent evidence also suggests that this specimen possessed a retained deciduous canine, which may have contributed to the levels of calculus present within this individual[5]. The location of these remains is currently the Museo Nacional de Ciencias Naturales de Madrid, although the final destination will be the Museo Arqueologico de Asturias, in Oviedo.

The dental calculus sample obtained from a Neandertal found in Breuil Grotta in Italy has been dated at 36,600 yBP and has been described previously[6]. The supragingival sample was removed from the lower left M2 occlusal tooth at the University of Florence in Florence, Italy, although the molar is currently stored at the Istituto Italiano di Paleontologia Umana Roma.

Non-human Primates

Calculus from three different adult non-human primates, including a chimpanzee, macaque, and baboon, were obtained from the Odontological Collection at The Royal College of Surgeons, London. The chimpanzee calculus sample (ACAD 12873) was obtained from an individual that had been shot in the wild in Sierra Leone in 1948. The macaque and baboon samples are from unknown provenance. The macaque and baboon specimens were unique within the museum, so it is likely they came from personal collections or were even living in captivity within England at the time of death. None of the non-human primates had signs of oral disease or caries, although the size of calculus between teeth and between individuals varied wildly.

Sudanese skeletons

Dental calculus was removed from two skeletons excavated at Al Khiday 2, a site located along the White Nile in the Sudan (16D4, grave 93 and 96). Both specimens are female and full length descriptions have been provided previously, although these samples do not have radiocarbon dates[7]. Briefly, the skeletons are Neolithic (mid 5th Millenium BC) and form part of an assemblage of 190 individuals excavated from a multi-period cemetery. The Neolithic skeletons were found in shallow circular pits. At this site, pots and ornamental objects were found in some graves, which were culturally associated to the El Shaheinab phase[8]. The Neolithic groups along the Nile Valley are thought to be pastoralists, but there is little information about their diet, as no well-preserved settlements have been found. Faunal remains of domestic and wild animals[9] were accompanied by both wild and domesticated cereals, such as wheat and barley[10], and were found in funerary contexts, suggesting a mixed diet. This diet likely supported the extensive calculus formation identified on these two Sudanese skeletons[7].

South African skeletons

The eight individuals from South Africa included within this study were taken from a series of over 40 Later Stone Age (LSA) skeletons stored in the Department of Human Biology of the University of Cape Town[11]. All skeletons are from the Western Cape Province, and the only selection factors were a radiocarbon date older than 350 yBP and the presence of significant calculus deposits on the teeth.

The eight individuals selected were divided into two groups based on the age of their skeletons. South African samples from the Pastoralist Period (AfrPP) AfrPP1 (UCT 587), AfrPP2 (UCT 67), and AfrPP3 (UCT 157) are all less than 1,000 years

old, while the other group of African hunter-gatherers (AfrSF) included seven individuals, who are all older than ~2,000 years (AfrSF). The oldest specimen was AfrSF2 (UCT 373), who died just short of 4,000 years ago. All ten individuals had advanced occlusal wear on the teeth, and all but AfrPP3 (UC 157) had heavy or extremely heavy wear on the incisors.

South African Specimens >2,000 yBP (AfrSF)

All of these individuals died more than 2,000 yBP, and are from coastal or adjacent areas ranging from the Cape Peninsula in the south to Elands Bay, about 200 km north of Cape Town, South Africa. All are from hunter-gatherer contexts, as pastoralists did not enter the region until 2,000 yBP[12,13]. The five individuals are female, and all exhibit advanced occlusal tooth wear, although the general data health pattern is better than the Pastoralist Period group. Only two individuals had initial caries in the enamel, and both instances were relatively minor. Furthermore, no teeth had been lost antemortem.

This is oral health pattern is consistent with an active foraging lifestyle with limited access to simple starches and free sugars[14], and where the teeth are cleaned mechanically by chewing of high fibrous content food. All of the hunter-gatherers within this collection that had dental calculus were women, potentially indicating a sex based difference in calculus formation, potentially explained by the female dental masticatory regime. In historic Kalahari hunter-gatherers, women continually sample nuts, berries, and roots as they gather food during the day[15], which might result in increased rates of dental calculus.

South African Pastoralist Period Samples (AfrPP)

These individuals all died roughly between 800 and 600 yBP and lived on the south coast of the province or in the neighbouring hinterland. AfrPP1 (UCT 582) was a woman from a pastoralist (as opposed to a hunter-gatherer) group, but would still be considered from the LSA in terms of technology[16]. This female individual had one carious premolar, had lost both lower first molars antemortem, and had a severe abscess in the region of the mandibular third molar. Next, AfrPP2 (UCT 67) was a male, but there is no archaeological information to confirm the lifestyle of this individual. AfrPP2 (UCT 67a) also had extensive periodontitis and had lost five teeth from the left side of the maxilla before death. A third sample AfrPP3 (UCT 157) within the Pastoralist Period group was initially analysed, but did not pass bioinformatic filtering due to the low numbers of identified phyla. This specimen was also probably from a foraging community, although there is no archaeological information to confirm the lifestyle of this individual. AfrPP3 (UCT 157) had three carious teeth, one of which was extensively damaged with over half of the crown missing.

All of the Pastoralist Period African individuals showed relatively poor dental health. It is possible that agricultural foodstuffs were traded in from the Bantu-speaking groups to the east of the region who were settled in the area of the Transkei by 800 years ago[17]. The general pattern of tooth loss and decay is in stark contrast to that seen in regional hunter-gatherers. The number of teeth with caries accounts for 8% of teeth recovered for the three individuals, and this rises to ~20% if the antemortem losses are considered. This is well above the expected numbers seen in hunter-gatherers[18] and is more consistent with a diet consisting of a mix of gathered and agricultural foods. The relatively low fluorine levels on the south coast of the

Cape Province complicate this interpretation, as people raised in the region are generally more susceptible to dental diseases[18].

Post-Industrial Revolution German Samples

Dental calculus samples were obtained from Hettstedt, located within the Mansfeld district in Saxony-Anhalt, Germany. The Hettstedt cemetery was set up in 1853 and excavated by the State Office for Heritage Management and Archaeology Saxony-Anhalt and Heritage Museum, Halle, Germany in 2010. The 75 burials were osteologically analyzed in an unpublished Master thesis by Klapdohr *et al.* in 2013. Socioeconomically, the Hettstedtt population is characterized by the mining and metallurgical work in the town. At the beginning of the 19th century, the inhabitants died at an early age, and only 5-7 % of the population reached their 60th year. By the end of the 19th century, life expectancy increased noticeably, likely due to improved hygiene and dietary changes, as well as the replacement of gruel as the main dietary component with a combination of cereals, potatoes, and milk. In addition, tea, cocoa, sugar, and tobacco no longer were luxury goods available to the elite only, and sugar consumption rose markedly from 2.4 kg per capita from the year 1840 to 4.7 kg in 1861 and 7.3 kg in 1875[19].

For 63 out of the 75 Individuals (84%), dental pathologies could be evaluated. Tooth loss during life was considerably higher in women than in men (60.9% and 39.1%, respectively). Approximately 20% of the adults exhibited an intermediate to severe degree of dental plaque formation. On average, each of the 63 individuals exhibited 15 carious lesions. Caries frequency was 100%, and caries prevalence was over 50%. Even children and juveniles exhibited a large proportion of teeth with

dental caries. Their poor dental health can probably be attributed to mushy and sticky foodstuffs.

Section II: Additional Information

Sample Collection

Dental calculus samples were collected at the respective locations that housed the skeletal material (Table S1). First, the teeth were examined to identify the tooth with the largest calculus deposit. Once a ridge on the largest deposit was identified, the skeletal material was wrapped in aluminium foil, and the calculus was removed from a single tooth by applying pressure with a dental pick. The calculus from an individual tooth was then collected into the aluminium foil and poured into a labelled, non-breakable container for transport (*e.g.* a sterile plastic 2. mL screw cap tube or plastic bag). On average, each calculus sample was <0.01 gram and 2x3x2 mm in size. Photographs of representative calculus samples from each host species have been included for reference (Figure S1).

Figure S1 – Photographs of representative dental calculus samples prior to decontamination. A scale bar of 0.5 cm is included for reference.

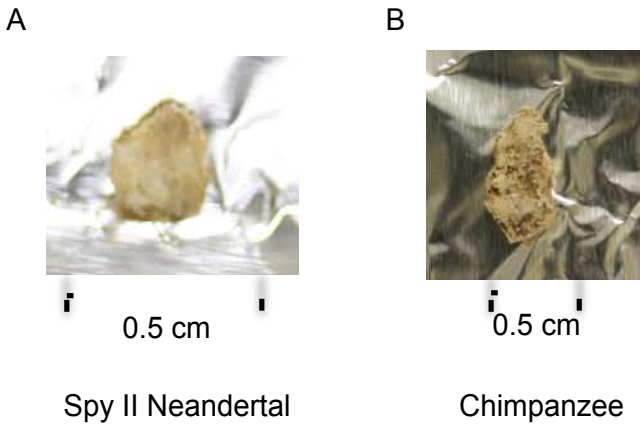

Sample preparation and DNA extraction

Upon arrival, all ancient samples were housed within a quarantine facility for ancient DNA research at The Australian Centre for Ancient DNA (ACAD) at The University of Adelaide, Australia. Before entry into the facility, sample containers were bleached and UV irradiated for 15 minutes to minimize exogenous microbial contamination. Samples were then stored at 4°C until DNA extraction was performed.

Prior to extraction, each sample was subjected to stringent decontamination procedures to reduce environmental contaminant DNA present on the outer surface of the dental calculus. The decontamination procedure is as follows. Each sample was individually placed in a sterile plastic dish and exposed to UV radiation for 15 minutes on each side. Next, the sample was submerged in 5% bleach and then purified water for 5 min, followed by immersion in 90% ethanol for 3 minutes to remove any residual bleach. The sample was then air dried for 5 minutes within a sterile container and then transferred to a sterile plastic bag. While inside the bag, the calculus was pulverized with a steel hammer. The corner of the plastic bag was then removed, and the sample was poured into a sterile 2 mL screw cap tube.

Once the powder was collected, DNA was immediately extracted as previously described, with the following modifications[20]. Briefly, samples were de-calcified by adding the powderized sample to a sterile tube containing 1.8 mL of 0.5 ethylenediaminetetraacetic acid (EDTA), 100 µL of 10% sodium dodecyl sulphate (SDS), and 20 µL of 20 mg/mL proteinase K and left to rotate at 55°C for 20 hours. Modern samples were extracted using the same protocol in a modern DNA lab at the University of Adelaide, but the resulting DNA (from modern samples only) was sheared according to manufacturer's recommendations to ancient DNA-like sizes (~150 bp) via a Covaris sonication system prior to shotgun library preparations.

Extraction blank controls (EBCs) were included at the beginning and end of each sample series (at approximately a ratio of one EBC per ten samples). Two empty tubes were included as EBCs in each extraction; these tubes were treated as if it were a powderized calculus sample. Released DNA was then bound to silica with 3 mL of modified QG buffer (Qiagen) as previously described[20], pelleted, and washed twice in 80% ethanol. Next, the cleaned and dried silica was resuspended in 100 μL of Tris-HCl buffer twice to elute the DNA. Eluted DNA was aliquoted and stored at -20°C until amplification. Notably, all the DNA and RNA-free certified water (Invitrogen Ultrapure distilled water) used to create the reagents was opened fresh or was frozen upon aliquoting to prevent microbial growth and contamination.

DNA from calculus samples examined previously by Adler *et al.* was also included in this study (Table S1)[1]; these samples were amplified according to the protocol below. To compare extraction efficiencies, Late Medieval samples (ACAD 8812 and 8824) were extracted using both methods. The two different extraction methods produced bacterial OTUs that were not statistically different at the phyla level (Figure S2).

Figure S2 – OTUs post-filtering to test the impact of different extraction methods on retrieval of bacterial communities and investigate PCR bias during 16S metagenomic studies of ancient DNA on a Medieval (Jewbury), Neandertal (Neandertal Spy I), ancient hunter-gatherer (Mesolithic Poland) or a chimpanzee (Chimpanzee) sample. A comparison between Late Medieval samples extract using two methods was examined, and three different cultures using either 37 cycles or 43 cycles of PCR under otherwise similar conditions was also examined.

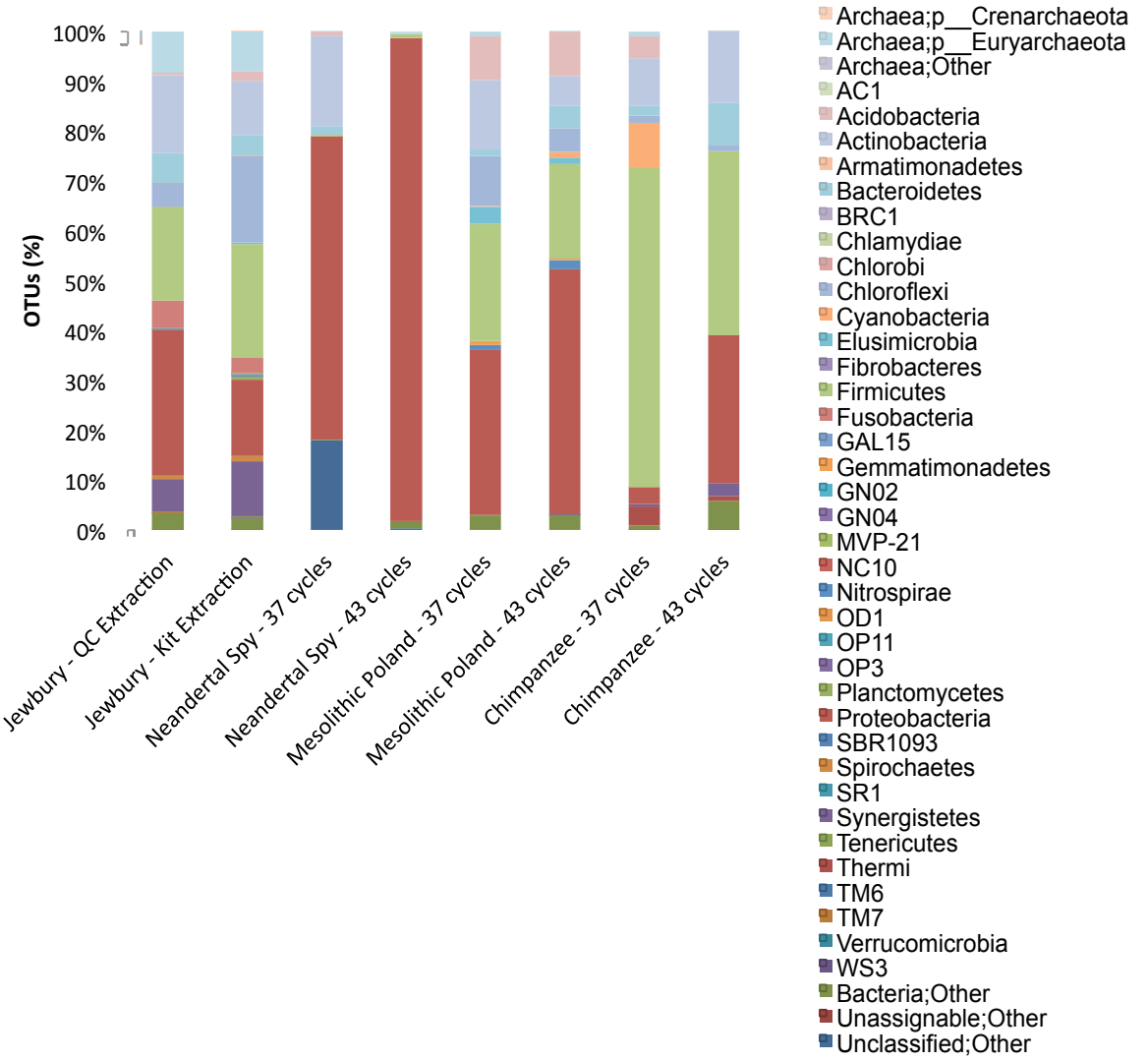

16S Ribosomal RNA Amplicon Library Construction and Analysis

Amplicon Library Preparation and DNA sequencing

The V4 region of the bacterial 16S ribosomal RNA (rRNA) encoding gene was targeted for amplification using degenerate Illumina fusion primers, as previously described[21]: forward primer 515F (AATGATACGGCGACCACCGAGATCTACA CTATGGTAATTGTGTGCCAGCM GCCGCGGTAA) and barcoded reverse primer 806R (CAAGCAGAAGACGGCAT ACGAGATnnnnnnnnnnnnAGTCAGTCAGCC GGACTACHVGGGTWTCTAAT)[21]. Each polymerase chain reaction (PCR) was prepared at ACAD, using ultraclean reagents and following strict ancient DNA protocols[22]. Each PCR tube contained 17.25 µL DNA-free water, 2.5 µL 10X ThermoPol Buffer (New England Biolabs), 0.25 uL HiFi Taq polymerase (New England Biolabs), 1.0 µL MgCL2, 1.0 µL of each primer, and 2.0 µL of genomic DNA, and each reaction was repeated in triplicate. Sealed reactions were then transported to a modern DNA laboratory at the University of Adelaide, and 16S rRNA targets were amplified under the following conditions: 95°C for 5 minutes; 37 cycles of 95°C for 0.5 min, 55°C for 0.5 min, 75°C for 1 min; and 75°C for 10 minutes. PCR products were cleaned (Ampure, New England Biolabs) to remove primers and enzymes, and DNA concentration was assessed (TapeStation, Agilent). Samples were pooled at equal nanomolar concentrations, and amplicons were sequenced on an Illumina MiSeq 2x150 bp kit using 12 bp custom indexes.

To determine if increasing the number of PCR cycles would increase DNA and OTU yield from ancient samples, a Spy Neandertal (ACAD 14017), European Mesolithic hunter-gatherer (12014 and 12017), chimpanzee (12873), and an extraction blank control (14022) sample were amplified for either 38 or 43 cycles under the same conditions. Increasing the number of PCR cycles significantly skewed

the bacterial communities observed within these samples (Figure S2). When amplicons were produced with 43 cycles of PCR, the Spy I Neandertal sample were dominated by Proteobacteria, and bacteria within other phyla became completely undetectable, such as Bacteriodetes (Figure S2). Although more DNA was amplified when the number of PCR cycles was increased, this analysis suggests that PCR bias due to increased amplification can significantly affect metagenomic analysis during ancient DNA studies, as expected[23,24]. Although increasing the number of PCR cycles may be required to amplify DNA from ancient samples of decreased quality and preservation, the minimum number of required cycles should always be utilized to decrease PCR bias.

16S rRNA Amplicon Bioinformatic Analysis

Two independent sequencing runs generated a total of 14,644,648 DNA sequencing reads. Sequences were demultiplexed to sample-specific fastq files from input BCL files using the Illumina CASAVA pipeline (version 1.8.2). Overlapping forward and reverse reads were joined (based on a maximum of 5% nucleotide difference over a minimum 5 bp overlap) using fastq-join[25], and singletons remaining after joining were discarded. Sequences were then trimmed using CutAdapt[26], and subsequent files were converted to QIIME-formatted fasta files using a publically available script from G. Watts (available here: http://www.u.arizona.edu/~gwatts/azcc/QIIMEfastaFormatter.pl). An average of 246,427 sequences/sample were then uploaded into QIIME (MacQIIME v1.5.0), a bioinformatics pipeline-based software for the analysis of metagenomic data[27]. OTUs were determined by clustering at 97% similarity in UClust[28], and representative sequences (first or cluster seed) were selected for each cluster. By default, clusters with less than five sequences were eliminated from the analysis. Lastly, 16S

sequences were given taxonomic assignments using the Greengenes database (v13) with the default setting (0.8)[29,30]. After singletons were removed, over 29,000 OTUs were observed using this approach prior to filtering, indicating that DNA damage and contamination could be inflating the number of observed OTUs, as expected[31].

Many of the ancient individuals analysed in this study, including the Spy and El Sidron Neandertals, historic primates, and ancient humans, have been stored in museum collections for long periods of time. In addition to microorganisms introduced through the soil, it is also possible that microbial contaminants are introduced during museum handling and storage or during site excavation. For example, Spy cave was excavated in 1886, and since that time, nearly all of the biological samples and archaeological remains from that site have been stored in museums, handled by scientists, and exposed to numerous storage boxes and facilities. Sequencing soil from Spy cave to analyse environmental contaminants is also is also problematic, because there are no available soil samples from the layers where the bones were collected due to the considerable length of time that has passed since the excavations. However, mammalian bones from the Spy site have been tested for DNA leaching from other bones in the site, and no evidence was found for DNA leaching within the cave[32]. Environmental exposure, sampling handling, and storage are significant issues when conducting ancient metagenomic research, and in this study, we have applied all currently available precautions to eliminate and examine this contamination within these ancient metagenomes. However, further assessment criteria, improved laboratory methods, and new bioinformatic tools should be developed to aid in this process.

Therefore, we considered and accounted for two types of contamination in our downstream analysis for both the 16S and shotgun data sets: environmental/museum

contamination and laboratory/reagent contamination. To account for environmental and museum contamination, we decontaminate the outer surface of the sample by both UV treating the sample and decontaminating this in bleach. To assess the contributions of laboratory contamination, we filtered the datasets for any taxa (eukaryotic or microbial) that are observed in soils that are analogous to that at archaeological sites. Previous publications have shown that environmental contamination, if present, leaves a unique signal microbial within the calculus[1,31]. To some extent, this signal can be identified and either analysed or removed from the dataset.

An initial analysis of 16S OTUs revealed taxa associated with laboratory contaminants and the environment were present in all calculus samples, including modern calculus samples. As is common in ancient DNA analysis protocols[33] and as has been recently recommended by Salter *et al*.[34], a conservative filtering regime was applied to identify and remove all of these contaminants from each sample. Extraction blank controls (EBCs) were included during the DNA extraction steps. EBCs were generated by including blank tubes during the demineralization step and were subjected to all of the reagents and processes that each ancient DNA sample undergoes. Therefore, sequences in EBCs are indicative of contaminant DNA present in the laboratory environment, reagents, and plasticware. Two EBCs were included for each DNA extraction that occurred for this project. Sequences from each EBC also underwent the same quality filtering, trimming, and OTU (taxa) selection process as reads present in ancient and modern DNA samples. Taxa identified within EBCs were present in higher proportions in ancient samples, likely due in part to the age and preservation of DNA within those samples (Table S2). After OTUs had been identified for all the samples and EBCs collectively, any OTU identified in any EBC

sample was removed from the ancient and modern samples. For example, if there were 10 reads for OTU 1 in Sample 1, and 5 reads for OTU 1 in an EBC sample, all 10 reads matching to OTU 1 were removed from Sample 1, as well as any other sample containing OTU 1. Because this step was done post-OTU identification, whole OTUs were removed, rather than the number of reads. If a specific *Staphylococcus aureus* OTU was identified in an EBC, then the specific OTU that matched that *S. aureus* OTU was filtered out from the ancient and modern calculus samples. This does not mean that all OTUs identified as *S. aureus* were removed.

Table S2 – The number of OTUs is monitored throughout the filtering process. The total number of reads removed and the percent of total reads discarded is displayed for each filtering step. Samples that did not meet the OTU threshold and were removed from downstream analysis (red) (SI Figure 4), while other samples were removed due to lack of accurate provenance or excluded because they were included as methodological replicates, but were retained in the SI figures and analysis for reference (orange).

SampleName	Cleaned/Raw Reads	Reads Post EBC Filtering	% Reads Discarded	Reads after Soil Filtering	% Reads Discarded	Reads after known contam filtering	% Reads Discarded	Total Reads Filtered	Total Reads (Oral)	Total % Reads Filtered
LBKS3	1449685	286341	80.2	281959.0	1.5	281308	0.2	80.6	162454.0	88.8
Chimp	791712	42505	94.6	42445.0	0.1	41182	3.0	94.8	32498.0	95.9
AfrPP1	778898	69025	91.1	69000.0	0.0	60480.0	12.3	92.2	49675.0	93.6
AfrSF5	596701	48042	91.9	48025.0	0.0	17586	63.4	97.1	17563.0	97.1
AfrSF4	474139	4783	99.0	4767.0	0.3	3732	21.7	99.2	3705.0	99.2
Neandertal – Spy I	462176	7778	98.3	7757.0	0.3	6670	14.0	98.6	5398.0	98.8
EuroHG2	419370	65876	84.3	64625.0	1.9	62309.0	3.6	85.1	39073.0	90.7
EuroHG1	409017	39170	90.4	39162.0	0.0	28749	26.6	93.0	26047.0	93.6
AfriPP2	380802	32062	91.6	31503.0	1.7	31336	0.5	91.8	22293.0	94.1
Modern C7	366603	45541	87.6	44648.0	2.0	44643	0.0	87.8	43291.0	88.2
IndRev1	346510	45080	87.0	44542.0	1.2	44518	0.1	87.2	32856.0	90.5
Modern C5	291597	46174	84.2	45824.0	0.8	45815	0.0	84.3	44444.0	84.8
IndRev2	284655	47278	83.4	46282.0	2.1	46260	0.0	83.7	42171.0	85.2
LBKS1	284453	37351	86.9	37134.0	0.6	35198	5.2	87.6	23853.0	91.6
LM5	283204	38482	86.4	38057.0	1.1	38046	0.0	86.6	18538.0	93.5
LM3	272488	19536	92.8	19358.0	0.9	19352	0.0	92.9	12195.0	95.5
BB	266414	11391	95.7	11233.0	1.4	11192	0.4	95.8	7400.0	97.2
Modern C6	261108	43404	83.4	42910.0	1.1	42903	0.0	83.6	42049.0	83.9
Modern C10	242510	29261	87.9	28922.0	1.2	28917	0.0	88.1	28248.0	88.4
Modern P2	239966	13416	94.4	13377.0	0.3	13371	0.0	94.4	13145.0	94.5
LM1 (QG)	239925	53686	77.6	52803.0	1.6	52792	0.0	78.0	39935.0	83.4
EuroHG 1 (43)	237920	6438	97.3	6426.0	0.2	5729	10.8	97.6	5430.0	97.7
BA2	235263	10133	95.7	9987.0	1.4	9967	0.2	95.8	7013.0	97.0
Modern P8	233069	40187	82.8	40006.0	0.5	39999	0.0	82.8	39812.0	82.9
EM4	225985	15296	93.2	15191.0	0.7	15178	0.1	93.3	5392.0	97.6
LBKS2	217339	27787	87.2	27577.0	0.8	27326	0.9	87.4	19246.0	91.1
LBKS4	213285	26128	87.7	25858.0	1.0	25819	0.2	87.9	15204.0	92.9
AfrSF3	212040	33494	84.2	32842.0	1.9	32783	0.2	84.5	26569.0	87.5
EM3	211172	32321	84.7	32063.0	0.8	32042	0.1	84.8	14708.0	93.0
AfrSud2	203867	20104	90.1	20097.0	0.0	18365	8.6	91.0	6791.0	96.7
LBKH2	200689	7556	96.2	7439.0	1.5	7419	0.3	96.3	5940.0	97.0
IndRev3	200329	30921	84.6	30415.0	1.6	30410	0.0	84.8	27084.0	86.5
Modern P7	194582	20833	89.3	20679.0	0.7	20676	0.0	89.4	20441.0	89.5
EuroHG2 (43)	193317	22684	88.3	22651.0	0.1	19781	12.7	89.8	14655.0	92.4
BA1	184631	9952	94.6	9822.0	1.3	9788	0.3	94.7	7258.0	96.1
Modern P6	180900	14634	91.9	14586.0	0.3	14577	0.1	91.9	14367.0	92.1
Chimp (45)	180498	6537	96.4	6524.0	0.2	6173	5.4	96.6	5517.0	96.9
LNBA	177184	12549	92.9	12441.0	0.9	12304	1.1	93.1	5118.0	97.1
AfrSud1	172206	2255	98.7	2219.0	1.6	2018	9.1	98.8	1971.0	98.9
LBKH 1	166325	25925	84.4	25612.0	1.2	25530	0.3	84.7	8860.0	94.7
LM2 (QG)	158464	23800	85.0	23585.0	0.9	23582	0.0	85.1	17413.0	89.0
Neandertal – Spy II	158142	988	99.4	977.0	1.1	568	41.9	99.6	556.0	99.6
Modern P10	158090	36626	76.8	36539.0	0.2	36536	0.0	76.9	35926.0	77.3
LM11	154101	11424	92.6	11329.0	0.8	10998	2.9	92.9	7752.0	95.0
EM1	149276	14466	90.3	14239.0	1.6	14201	0.3	90.5	9821.0	93.4
LM1	146117	17670	87.9	17468.0	1.1	17463	0.0	88.0	11568.0	92.1
Macaque	143906	34161	76.3	33877.0	0.8	33786	0.3	76.5	24194.0	83.2
Tooth	130802	26018	80.1	25613.0	1.6	25602	0.0	80.4	21864.0	83.3
EM2	125471	28996	76.9	28703.0	1.0	28692.0	0.0	77.1	16273.0	87.0
Neandertal - El Sidron 2	120468	8428	93.0	8404.0	0.3	6761	19.6	94.4	6229.0	94.8
AfrSF2	112315	425	99.6	422.0	0.7	277	34.4	99.8	265.0	99.8
LM2	96682	11413	88.2	11171.0	2.1	11159	0.1	88.5	5925.0	93.9
Neandertal - El Sidron 1	3446	1467	57.4	1463.0	0.3	1411	3.6	59.1	487.0	85.9
Baboon	38	4	89.5	4.0	0.0	4	0.0	89.5	4.0	89.5
AfriPP3	26	1	96.2	1.0	0.0	1	0.0	96.2	1.0	96.2
AfrSF 6	17	7	58.8	7.0	0.0	7	0.0	58.8	4.0	76.5

Each of the extraction blanks contained different OTUs, likely stemming from the different extraction dates over the course of this project. Nevertheless, the six most abundant OTUs were classified as Comamondaceae, Pseudomonadaceae, *Acinetobacter, Comamonas*, *Tepidimonas*, and *Burkholderia,* and were similar to published findings[34]. The removal of the OTUs from EBCs within each sample removed an average of 87.2% of the total reads from each ancient 16S rRNA calculus sample data set, suggesting that ancient samples contain large levels of laboratory contamination (Table S2). Although the quantity of reads removed from the calculus samples was high, this was not unexpected[34]. This is typical within ancient DNA studies, as background contamination from laboratory reagents can swamp out the ancient sequences available within an ancient DNA extract. Laboratory contaminants can similarly plague modern amplicon based metagenomic studies, as an increase in endogenous signal was observed when OTUs from EBCs were removed from an analysis[35]. In this study, removing EBC OTUs is an essential step to remove the noise and increase the endogenous signal for downstream phylogenetic and comparative analysis, especially within ancient samples that can be easily overwhelmed with modern DNA contaminants.

Next, to address possible environmental or soil contamination in ancient samples that have been buried or recovered from the ground, OTUs identified in temperate coniferous forest soil were additionally removed. Six fna files corresponding to coniferous forest soil samples were downloaded from MG-RAST (mgrast_ID: mgp72) and analysed in parallel with calculus samples[36]. These soil metagenomes were selected for experimental continuity (*i.e.* amplification of identify 16S V4 region) and similarity to the archaeological sites examined in this study (*i.e.* temperate forest), as no experimentally similar cave soil data sets were available when

this analysis was completed. OTUs from the soil data set were extracted and subsequently filtered from the already EBC-filtered data, as earlier described. On average, 1% of OTUs corresponding to soil were removed from the EBC-filtered data (Table S2), suggesting the ancient samples are not highly contaminated with environmental soil DNA or, more likely, that strict sample decontamination procedures prior to extraction minimize soil DNA contamination.

Finally, common laboratory contaminants were also removed. Several bacterial genera have been repeatedly detected within bacterial DNA extraction kits, enzymes, and reagents[34]. Therefore, these genera were additionally filtered from our analysis: *Acidovorax, Acinetobacter, Aeromicrobium, Afipia, Bacillus, Bradyrhizobium, Brevibacillus, Brevibacterium, Burkholderia, Caulobacter, Delftia, Devosia, Herbaspirillum, Lamia, Mesorhizobium, Methylobacterium, Ochrobactrum, Olivibacter, Paenibacillus, Pedobacter, Propionibacterium, Pseudomonas, Pseudoxanthamonas, Ralstonia, Rhizobium, Rhodococcus, Sphingomonas, Stenotrophomonas,* and *Sulfuritalea*. While most of these OTUs had been removed in the previous EBC OTU filtering step, on average an additional 5.3% of the EBC- and soil-filtered reads were removed. The number of reads removed from each sample was higher in the ancient samples, as expected (Table S2). After this filtering, each sample contained an average of 19.4 thousand reads.

Upon removal of environmental and laboratory contaminants, there were several samples with lower numbers of reads (<500 reads) that also contained only a few bacterial phyla (<3 phyla). The low bacterial diversity likely signifies that the remaining reads do not represent an intact oral bacterial community. Therefore, four samples were excluded from downstream analysis, which resulted in the removal of three South African individuals (AfrPP3, AfrSF1, AfrSF5) and the baboon.

Nevertheless, over 775 different OTUs were detected using this method, and 30 different OTUs were present within all of the cultures examined. In addition, filtered modern calculus samples were comparable to oral bacterial communities identified by Adler *et al*.[37] and the Human Oral Microbiota Database (HOMD)[38], while remaining distinct from environmental controls, including soil, sediment, water, and an archaeological tooth sample, as shown by Adler *et al*.

Shotgun Metagenomic Library Construction and Analysis

Shotgun Metagenome Library Construction

Shotgun metagenomic libraries for new samples collected in this study were constructed as previously described for ancient DNA research[20,39], with the following modifications. Briefly, 20 µL of DNA was polished in 20 µL reaction with T4 polynucleotide kinase (New England Biolabs) and T4 DNA polymerase (New England Biolabs) for 15 minutes at 25°C. Reactions were cleaned using a MinElute Reaction Cleanup kit (Qiagen). Truncated Illumina adapter sequences with 5 bp unique barcodes[39] were ligated onto double stranded DNA molecules using T4 DNA ligase (Fermentas) for 60 min at 22°C. After a clean-up using a Qiagen MiniElute Reaction Clean-up kit to removed excess ligase, adapter sequences were filled using a Bst DNA polymerase (New England Biolabs) for 30 minutes at 37°C, followed by denaturation of the polymerase at 80ºC for 10 minutes. The resulting reaction was then used as a template in five independent PCR reactions (12 µL DNA-free dH_20, 2.5 µL 10x buffer, 2.5 µL 25 mM $MgCl_2$, 0.25 µL 25 mM dNTPs, 1.25 µL of IS7 and IS8 primer sequences[39], 0.25 µL HiFi DNA polymerase, and 5 µL of the Bst reaction mixture) under the following conditions: 12 min at 94°C; 13 cycles of 30 sec at 94°C, 30 sec at 60°C, 45 sec at 72°C; and 10 min at 72°C. PCR reactions were pooled and

cleaned using Ampure PCR purification (Agencourt). Libraries were then re-amplified with the same conditions using GAII indexing primers[39] to include a single P7 (3') index sequence unique to each sample, re-pooled, and cleaned again using Ampure. Libraries were quantified using a TapeStation and quantitative PCR (KAPA Illumina quantification kit) and pooled at equimolar concentrations prior to paired-end sequencing on an Illumina HiSeq (Neandertals; chimpanzee; modern human) and NextSeq (all other remaining samples).

Shotgun Metagenomic Bioinformatic Analysis

Raw fastq files obtained from either sequencing machine were demultiplexed using Sabre 1.0 (available here: https://github.com/najoshi/sabre) according to sample specific index sequences, and reads were then merged using bbmerge (available here: http://sourceforge.net/projects/bbmap/). Adapter removal was then used to identify reads that matched both the 5' and 3'barcode sequences (5 bp) and trim both the barcode and adapter sequences from the reads. Taxonomic identifications of collapsed (merged) reads were identified using MALTX, as non-merged reads were greater than 300 bp in length and likely represent more contamination than endogenous signal. Briefly, MALTX (v0.0.12) was developed by the Huson lab at the University of Tuebingen and is an in-house Java program that compares DNA reads against a protein reference database, such as NCBI-nr[40]. It employs a seed-and-extend strategy using spaced seeds and a reduced alphabet in the seed step, similar to DIAMOND[41]. MALTX employs the same spaced seeds, reduced alphabet, and alignment strategies as DIAMOND but uses a hash-table rather than double-indexing to find seed matches between queries and references. The output of both programs is similar, but not identical, due to differences in the heuristics used. MALTX output files were converted into rma files and uploaded into MEGAN5[42]. Species identified in EBC and

environmental (water and soil) controls were removed from calculus samples in MEGAN5; sequences identified at higher-level classifications in the control samples were not removed from the data, due to unknown provenance. Briefly, species identified in EBCs or environmental controls (Extended Data Figure 6A) were selected (Select>Leaves) from all calculus samples. The inverse of these species (*i.e.* all taxa not selected) were then exported into a new file, conserving all species not identified in controls and any higher order taxa. This data file was then utilized for downstream analysis.

In MEGAN5, alpha diversity was conducted on the filtered data set by calculating both Simpson's and Shannon's inverse indexes from all taxa, while beta diversity was examined by calculating the Euclidean and Bray-Curtis distances of the genera identified in each sample. UPGMA clustering of distances was performed in SplitsTree[43], and tree construction was visualized and edited in FigTree v1.4.1 (available at: http://tree.bio.ed.ac.uk/software/figtree/). GraftM was employed to identify sequences corresponding to the 16S ribosomal RNA encoding genes (available at: https://github.com/geronimp/graftM). These sequences were selected by a hidden Markov chain model in hmmer against the RDP database to ensure eukaryotes were distinguished, and identified by their placement into a phylogenetic tree using pplacer. Metagenomic and 16S rRNA compositions were compared to GraftM analysis by normalizing the taxonomic classifications across NCBI, RDP, and Greengenes identifications to the NCBI convention during downstream analysis in MEGAN5. Statistical analysis of shotgun data was completed using LefSe[44].

Genomic and Phylogenetic Analysis

Patterns of DNA damage were plotted from shotgun sequencing for several species. First, species of interest, including modern oral, respiratory, and gut

pathogens, were identified from the MALTX output. Collapsed reads from each species were then mapped to the identified reference genome with BWA v0.6.2 [45], using the parameter space recommended for ancient DNA (no seed, one gap opening, relaxed edit distance)[46]. Duplicate reads were removed using FilterUniqueSAMCons.py[47]. For example, MALTX identified the highest number of archaeal sequences as matching to *Methanobrevibacter*, so both the gut and oral *Methanobrevibacter* genomes were used independently as a reference sequence to map any and all reads from fastq files. Reads aligned to either genome were then analysed in MapDamge 2.0.2[48]. Once the correct reference was identified (*i.e.* whichever reference genome matched the most sequences), the identification of genes present in the modern genome, but putatively absent in the ancient genome (*i.e.* no reads mapping to the reference loci), were completed by comparison in Geneious[49]. Plots of G/C content and mapped genomic regions were constructed using Circos[50].

Next, phylogenetic relationships between ancient bacterial species and modern relatives were assessed. All available published genomes and whole genome sequences of the identified species and closely related taxa were obtained from NCBI, and aligned using default parameters in progressiveMauve[51]. Outputs files were converted into a fasta format using bx-python scripts (available at: https://github.com/bxlab/bx-python). Dissimilar and poorly aligned sections from these genomes were removed using GBlocks[52]. Phylogenetic trees of the aligned sequences were estimated using the maximum likelihood (ML) procedure in RAxML v 8.1.21[53] using the GTRGAMMA substitution model. The best ML tree was retrained from 20 ML computations, and support values were obtained from 100 bootstrap replicates using the rapid bootstrapping algorithm[54]. Divergence times between closely related strains (*i.e. M. oralis* and *M. smithii*) were estimated using the

Bayesian Markov chain Monte Carlo procedure available in the BEAST package[55]. We used both strict and relaxed (uncorrelated lognormal) molecular clock models, and we assessed sufficient sampling by verifying that the effective samples size of all parameters was at least 200. Finally, we calculated the ratio of non-synonymous to synonymous nucleotide substitutions per site (d_N/d_S) for the ancient and modern *M. oralis* strains. We selected the genes that corresponded to protein coding regions and transcribed them using the bacterial, archaeal, and plant plastid code as implemented in BioPython[56]. If stop codons were identified in the ancient strain, which might occur due to reading frame shifts or particular features of the archaeal genome, the coding sequence was removed. Of the 1990 gene identified, 375 genes met these criteria. We then used a custom script (available at https://github.com/sebastianduchene/adna_dat) to calculate the number of non-synonymous and synonymous substitutions, as our analysis was restricted two sequences (the only available reference sequence and the ancient genome; raw count), which precludes the use of more sophisticated codon substitution models. A cut-off value of 0.1 was utilized to identify genes under purifying selection, while a cut-off of 1 was utilized for genes under positive selection.

Dietary Analysis

The shotgun data set was also examined for eukaryotic sequences that could be indicative of dietary food sources. While eukaryotic sequences represented a small fraction of the total reads, sequences pertaining to food sources could still be identified. However, several initial results seemed spurious (*i.e. Drosophila* or *Xenopus* in the modern human). To remove spurious results, we removed reference genomes that contained known levels of human DNA contamination[57,58]. This filtered many of the spurious results with the exception of ticks in the modern human (Table

549 1). The tick genome was not included in published analyses that examined human
550 DNA contamination within genomes, so the validity of this finding is insecure. It is
551 highly unlikely that this modern individual was eating ticks, and more likely
552 represents unidentified contamination in the tick genome that originates from either
553 human or microbial DNA. Similarly, the Spy I Neandertal also contained hits to many
554 spurious results, which also likely arise from modern contamination. Regardless,
555 dietary analysis from dental calculus is a burgeoning new field, and accurate reference
556 genomes that reflect ancient taxa are very limited. As damage patterns could not be
557 investigated due to the limited number of hits, we must note the limitations of the
558 current approach. In this study, we have assumed that hits to known related modern
559 species equate with related ancient taxa. However, this is a large assumption, and
560 further investigation using enrichment hybridization techniques or deeper sequencing
561 will help verify these results. There is also always a possibility that these results
562 represent contamination, resulting from DNA leaching in groundwater, sample
563 mixing during archaeological excavation, or DNA contamination from the adhesive
564 used to assemble ancient skeletons. Certainly, further research and development of
565 dietary calculus tools are needed to fully verify the limited dietary findings reported in
566 this study.

Additional Results

Amplicon Sequencing Analysis

16S rRNA SourceTracker Analysis

To explore bacterial contaminants and the impact of quality filtering on the16S rRNA data set, the raw (pre-filtering) and filtered sample OTU tables were analysed using the take-one-out method in SourceTracker 0.9.6[59]. Comparison samples (human skin and gut, soil, outdoor air, and indoor air microbiota) available with the Source Tracker package were used to identify the source of contamination introduced into ancient samples. To ensure EBC and negative-template PCR control contamination was effectively removed during the filtering process, EBC and PCR negative samples were also used as comparison samples. OTUs present in less than one percent of samples were also removed to increase computational speeds[60], and sample groups (cultures) that contained only one sample were excluded in the take-one-out analysis. The results were averaged across all samples per group, and the proportions were attributed to non-oral human microbiota, soil, and indoor/outdoor air. OTUs falling within the SourceTracker default "Unknown" category were collapsed into a single value ("Other").

As expected, the raw data (Extended Data Figure 3A) showed a mixture between cultures, compared to the filtered data (Extended Data Figure 3B). This indicates shared sequences exist between all samples in the raw data and likely represent laboratory contamination. Indeed, these sequences were removed during the filtering process. Hence, filtering enhances signal within groups and highlights the importance of tracking and removing contaminating sequences from sequencing data. It is interesting to note that more ancient/poorly preserved samples (Neandertal and African samples) contained increased proportions of contaminant reads attributed to

592 the EBC and PCR negative samples, likely due to preservation bias. Higher
593 contamination levels would be expected in older samples, because the endogenous
594 DNA proportion typically decreases with samples age[61]. As expected, the filtered data
595 shows no overlap of sequences between the EBC and PCR negative samples with the
596 calculus samples. Additional non-oral bacterial communities were collapsed into a
597 single category ("Other"), as no calculus sample (raw or filtered) had derived
598 sequences from these groups. This demonstrates that the non-oral bacteria identified
599 in ancient samples are unique and are not large components of the human mouth,
600 skin, or the environmental contamination examined here.
601 *16S rRNA Dissimilarity Analysis*
602 To identify unique OTUs and determine how they may contribute to
603 community-based phylogenetic analysis, dissimilarity indexes were first calculated
604 and compared for OTUs falling within the 99th percentile. Filtered OTU tables from
605 the calculus samples and EBCs were individually converted into a matrix using an in-
606 house python script and R[62]. Raw read within samples were counted, and the
607 maximum relative abundance was determined. The data sets were then filtered for
608 taxa that contained a proportion of >1% abundance, and the Jaccard dissimilarity
609 distance was calculated using the vegan package within R. Jaccard distance is based
610 on presence-absence similarity, in contrast to the abundance related measurements,
611 such as Bray-Curtis and Chao indices[63]. The abundance for each taxa >1% was
612 organized according to Jaccard similarity and placed in a heat map (Extended Data
613 Figure 2; Table S3). Taxa present at greater than 5% abundance were also identified
614 and flagged for display purposes as highly abundant OTUs. All R scripts to create
615 heat maps and Jaccard dendograms are available upon request.
616

Table S3 – The taxa identified at a greater than 1% proportion in each sample were grouped according to bacterial phyla,. The proportion of organisms in each phyla was reported in this chart. The two phyla with the highest number of organisms was determined, and the cell containing that information is highlighted below.

Bacterial Phyla	No-Agriculture	Agriculture	19th Century	Modern
Acidobacteria	0.02	0.05	0.21	0.06
Actinobacteria	0.1	0.41	0	0
Bacteroidetes	0.04	0.01	0.43	0.36
Chlamydiae	0.02	0	0	0
Chloroflexi	0.02	0.05	0	0
Elusimicrobia	0.02	0	0	0
Euryarchaeota	0	0.15	0	0
Firmicutes	0.36	0.14	0.14	0.15
Fusobacterium	0	0	0	0.26
Nitrospirae	0	0.01	0	0
Planctomycetes	0	0.01	0	0
GAL15	0.02	0	0	0
Gemmatimonoadetes	0.02	0	0	0
Plactomycetes	0.04	0	0	0
Proteobacteria	0.28	0.09	0.21	0.13
Spiroachaetes	0	0	0	0.02
Synergistetes	0	0.04	0	0
Unidentified	0.06	0	0	0

617

Utilizing these heat maps and Jaccard matrixes, four clusters were identified, which have been simplified as: No-agriculture (hunter-gatherers, foragers, and some pastoralists); Agriculture (early farming cultures); 19th Century (Industrial Revolution); or Modern (Extended Data Figure 2). Interestingly, a hunter-gatherer sample (EuroHG-2) fell intermediate between No-agriculture and Agriculture groups due to a single OTU (*Nitrospirales* sp.), which may reflect contact with contemporaneous agriculturalists or the transition to an agriculturalists based diet[64,65]. This may also demonstrate the lack of reproducible signal when analysing ancient amplicon data sets. This analysis highlighted several notable phyla-level patterns when the OTUs present at >1% were grouped into their respective phyla (Extended Data Figure 2; Table S3). Firmicutes and Proteobacteria were typically identified in ancient non-agriculturalists, while an increase in Bacteroidetes was observed in more modern samples (IndRev and modern). Fusobacteria were only identified as highly abundant in modern individuals. While potentially biological, these large-scale differences also appear to correlate with the age of sample and again highlight potential issues with utilizing >200 bp amplicons to analyse the genetic diversity within ancient samples.

Shotgun DNA sequencing analysis

Benchmarking MALTX Analysis

Species identification from diverse ancient metagenomic sequences is a difficult task, especially with fragmented and damaged DNA reads. While many ancient DNA studies have used BLAST-based metrics for species identification[66], large data sets require analytical software with rapid, accurate analysis methods. To examine how well MALTX performs relative to other rapid metagenomic analysis

643 tools (*i.e.* benchmarking), we created several *in silico* data sets from 49 bacterial
644 genomes of representative taxa previously detected in ancient dental calculus
645 genomes[1] (Table S4). To assess how MALTX would respond to short read lengths
646 versus damage introduced into ancient shotgun libraries, we simulated modern or
647 ancient (damaged) metagenomes using an average of 1 million reads per reference
648 genome at three average size length distributions (40 bp, 80 bp, and 120 bp),
649 generating six total simulated metagenome data sets. Modern simulated metagenomes
650 were constructed using ArtificialFastqGenerator[67] that simulated standard sequencing
651 errors. These simulated data sets were then subjected to damage (*i.e.* generated
652 damage within the data set) using an in-house program (SIMWRECK;
653 https://github.com/mtrw/simwreck) with the following parameters: p=3.35; d=0.3;
654 D=0.65. These simulated metagenomes were then analysed using default parameters
655 in MG-RAST[68] (best hit classification), DIAMOND[41], MetaPhylAn[69], and MALTX.
656 Simulated metagenomes could not be analysed in some situations due to size
657 fragment cut-offs (*i.e.* MALT and DIAMOND (40 bp) and MG-RAST (70 bp)).
658

Table S4 – Bacterial species identified from ancient dental calculus (Adler *et al.*, 2013) used to construct simulated metagenomes are listed.

Species genomes use to construct simulated metagenomes	Total number of sequences included	Percent of total metagenome
Agrobacterium tumefaciens 5a	2766360	3.82
Anaerolinea thermophila uni 1	1846052	2.55
Bacillus anthracis 52 g	2897088	4.00
Bacillus subtilis best7003	2323328	3.21
Bordetella pertussis 18323	1378624	1.90
Burkholderia cepacia gg4	2313732	3.19
Caldilinea aerophila dsm 14535 nbrc 104270	2441584	3.37
Campylobacter concisus 13826	1159324	1.60
Cardiobacterium hominis atcc 15826	1188668	1.64
Chlamydophila pneumoniae ar39	706596	0.98
Chlorobium limicola dsm 245	1520880	2.10
Enterococcus durans atcc 6056 ente dura atcc6056 v1	1709420	2.36
Escherichia coli e22	3044956	4.20
Fretibacterium fastidiosum	1021140	1.41
Fusobacterium necrophorum d12	1023220	1.41
Fusobacterium nucleatum 13 3c	1059856	1.46
Haemophilus aegyptius atcc 11116	1060140	1.46
Haemophilus haemolyticus hk386	1016300	1.40
Haemophilus influenzae 10810	1091756	1.51
Helicobacter pylori 2017	869468	1.20
Ignavibacterium album jcm 16511	1884708	2.60
Jonquetella anthropi e3 33 e1	831340	1.15
Klebsiella pneumoniae 120 1020	2673400	3.69
Lactobacillus acidophilus 30sc	1154960	1.59
Lactobacillus buchneri atcc 11577	1605508	2.22
Lactobacillus vaginalis atcc 49540	1031800	1.42
Leptotrichia buccalis c 1013 b	1109020	1.53
Listeria monocytogenes asm38292v1	1541648	2.13
Mycobacterium leprae tn	1604024	2.21
Mycobacterium tuberculosis 98 r604 inh rif em	1634900	2.26
Mycoplasma genitalium g37	281808	0.39
Neisseria bacilliformis atcc baa 1200	1103912	1.52
Neisseria gonorrhoeae 1291	1077240	1.49
Porphyromonas gingivalis atcc 33277	1331604	1.84
Prevotella denticola cris 18c a	1740700	2.40
Pseudomonas aeruginosa 18a	2203408	3.04
Pseudomonas fluorescens a506	2774324	3.83
Pyramidobacter piscolens w5455	1152084	1.59
Rhodobacter capsulatus b6	1384316	1.91
Staphylococcus aureus 04 02981	1412124	1.95
Staphylococcus caprae c87	1228496	1.70
Staphylococcus epidermidis 14 1 r1 se	1251648	1.73
Streptococcus mitis 11 5	1060000	1.46
Streptococcus mutans ua159	1100692	1.52
Streptococcus oralis atcc 35037 asm14856v1	1073252	1.48
Treponema denticola al 2	1539832	2.13
Treponema pallidum str fribourg blanc	622120	0.86
Yersinia pestis 113	2586256	3.57

659

Species identifications and community structures were influenced by analysis method, as expected[70]. In UPGMA clustering of Bray-Curtis distances, modern and simulated damaged metagenomes analysed in DIAMOND and MALTX clustered more similarly for all lengths, likely reflecting similarities in the heuristic algorithms employed in each method (Extended Data Figure 5B). MetaPhlAn results clustered to the exclusion of DIAMOND and MALTX outputs, and MG-RAST outputs clustered to the exclusion of all other data sets. MG-RAST analysis of ancient fragments was highly biased, and resulted in data that was indistinguishable across ancient and modern samples. Worryingly, the EBC samples also looked similar to modern calculus samples when analysed by MG-RAST (Extended Data Figure 4B). MG-RAST analysis is inherently limited by a 70 bp threshold for species identification and is therefore problematic to analyse ancient DNA data sets, as the average sequence size in the ancient data sets is less than 70 bp (Table S6). With the exception of the MG-RAST analysis that is biased towards larger fragments (>70 bp), taxonomic profiles constructed from each data set demonstrated similar trends (Extended Data Figure 5A). Interestingly, DNA damage had a larger impact on taxonomic identifications than DNA fragment length, although fragments <80 bp could not be included. DIAMOND and MALT were more accurate at maintaining taxonomic identifications even when damage was included in the analysis, in contrast to profiles generated from MetaPhylAn, which were highly impacted by damage and clustered separately rather than together during UPGMA clustering (data not shown). Overall, DIAMOND and MALTX better reflected unbiased bacterial community structure that was more similar to the input species and was more robust to biases introduced through different DNA fragment lengths and damage.

In addition, raw data for all of the available modern oral metagenome data sets (amplicon and shotgun) on the MG-RAST repository were downloaded and analysed by MALTX to identify similarities and differences between this analysis and published findings (Extended Data Figure 5C). Amplicon and shotgun genera were UPGMA-clustered according to Bray-Curtis distances. Modern calculus deeply sequenced in this study (described below) possessed bacterial phyla similar to plaque shotgun metagenome samples[71]. All plaque and calculus samples clustered to the exclusion of a tracheal metagenome[72], as expected. Salivary amplicon data analysed by MALTX were distinct from shotgun data, as expected; however, salivary data analysed by MALTX was similar to the common salivary microbiota and was stable through time, as expected[73]. Overall, MALTX was able to reconstruct published results, demonstrating its accuracy for diverse and ancient metagenomic samples.

Impacts of Filtering and Analysis Method on Shotgun Data

DIAMOND and MALTX (0.0.12) analyses yielded similar results (Extended Data Figure 6), but filtered DIAMOND data sets tended to have increased Proteobacteria proportions even in modern specimens (Extended Data Figure 6; Table S5 and S6). Because the majority of taxa within the EBCs were Proteobacteria, it is possible that laboratory and environmental contamination were not accurately removed using species-level DIAMOND identifications. Only sequences identified to the species level can be filtered from shotgun data, so the inability to identify specific species in either analysis method would allow more contaminant reads to infiltrate the data. Therefore, MALTX analysis was selected as the best approach and was utilized for all downstream analysis.

Table S5 – Shotgun metagenomic sequencing was performed on the following subset of samples, and the outputs were analysed using DIAMOND. The raw number of reads after demultiplexing is displayed, as well as the number of reads present after adapter trimming and filtering species that were identified within the EBCs.

	Raw Data	Post-Filtering	
Samples	**# Reads**	**# Reads**	**% Removed**
Chimp	18680535	17214005	8%
ElSidron1	56584638	49943977	12%
ElSidron2	66905980	47820005	29%
Spy I	69901550	3996189	94%
Spy II	87504507	17388077	80%
WarB61	94679298	945484	99%
WarG12	77177157	767283	99%
Modern	44000223	26735211	39%
EBC1	6350329	53309	99%
EBC2	663351	9070	99%
EBC3	238422	238395	0%
BraccWater	14533539	2383467	84%
GrndWater	76271556	8191610	89%
GrassSoil	93579626	35243604	62%
ForestSoil	50544126	6187071	88%
Total Reads	757614837	217116757	71%

Table S6 – 16S rRNA reads identified within deeply-sequenced shotgun datasets were identified by GraftM, and the average read length was calculated using the read_length.py script in bbmap.

	Total Reads	Maximum Length	Minimum Length	Average Length	Median Length	Mode Length
Chimpanzee	8639	166	44	75.4	70	60
El Sidron 1	20035	180	44	70.1	60	60
El Sidron 2	33042	181	44	74.8	70	60
Spy 1	7307	179	44	79.7	70	70
Spy 2	2256	141	49	89.6	70	60
Warinner B61	327	604	400	138.2	120	100
Warinner G12	232	431	100	137.3	120	100
Modern	33612	186	43	89.8	80	70

709

710 In addition to removing species identified in EBC samples, we also filtered
711 environmental species to assess environmental contamination and provide a primitive
712 way of estimating the 'endogenous' DNA present in a sample. We removed species
713 found in soil and water metagenomes from previously sequenced data sets available
714 in MG-RAST (MG-RAST IDs: 4536380.3, 4536373.3, 4516952.3, 4511193.3,
715 4477876.3) (Extended Data 6; Table S7). As stated in the main text, the Spy
716 Neandertal samples were drastically impacted by the lab and environmental filtering
717 (80-94% reads removed). This was in stark contrast to the El Sidrón samples (12-
718 29%), indicating that less contaminant DNA is present in the Spanish Neandertal
719 material. In anatomically modern human (AMH) samples, the impacts of filtering
720 were independent of sample age, as ~8,000 year-old AMH European hunter-gatherers
721 had no sequences removed, while contemporaneous European LBK samples had up to
722 70% of the sequences removed (Table S7). The extraction facility also appeared to
723 play a role in the level of background contamination present in the samples. For
724 example, two Medieval calculus samples processed by Warinner *et al*., contained
725 >99% background sequences, whereas the modern sample extracted in a modern
726 DNA facility at the University of Adelaide, Australia, had 39% of the sequences
727 removed from the data. The youngest samples processed in the ancient facility
728 (Industrial Revolution samples) both contained <2% background contamination.
729 Overall, this filtering process estimated that up to 24% of the total ancient sequencing
730 reads identified in this study are non-endogenous, in stark contrast to the 82.7%
731 identified in amplicon data sets.
732

Table S7 – The total number of reads analyzed by MALTX (nucleotide alignment) in each metagenomic sample was calculate prior to and after filtering species identified in QG extraction blank control reads and environmental samples (BraccWater, GrndWater, GrassSoil, ForestSoil) from ancient dental calculus samples.

Samples:	Raw Data # Reads	Post-Filtering # Reads	% Removed
Chimp	18680535	17214005	8%
ElSidron1	56584638	49943977	12%
ElSidron2	66905980	47820005	29%
Spy1	87504507	17388077	80%
Spy2	69901550	3996189	94%
EuroHG1	145907	145670	0%
EuroHG2	93208	93046	0%
EuroLBK1	132671	39379	70%
EuroLBK2	258241	125359	51%
EuroLBK3	346073	158045	54%
Sudan1	203099	5240	97%
Sudan2	284254	81138	71%
SouthAfr1	3649738	3390649	7%
SouthAfr2	654275	308064	53%
WarB61	94679298	945484	99%
WarG12	77177157	767283	99%
UrbMed1	197853	51720	74%
UrbWar2	187667	70906	62%
AfrPP2	1105368	820741	26%
AfrPP1	6292653	2641418	58%
IndRev1	116542	115772	1%
IndRev2	11702696	11435338	2%
Modern	44000223	26735211	39%
EBC1	6350329	53309	99%
EBC2	663351	9070	99%
EBC3	238422	238395	0%
BraccWater	14533539	2383467	84%
GrndWater	76271556	8191610	89%
GrassSoil	93579626	35243604	62%
ForestSoil	50544126	6187071	88%
Total Reads	309905088	236512864	24%

733

Diversity Analysis of Shotgun Data

To analyse species diversity through time, Shannon and Simpson-Weaver indexes were calculated from filtered (non-rarefied) shotgun data sets in MEGAN5 (Extended Data Figure 8). An earlier examination of Gram-positive microorganisms from ancient dental calculus identified a statistical decrease in species diversity over time[1], and decreased diversity has been reported in several studies examining the microbiota of greater apes compared to modern humans[74]. Statistical differences in diversity through time were not observed between samples of this study, although differences were observed in samples from this study compared to others from Warinner *et al.*[31] (Extended Data Figure 8). Due to the large differences in sequencing depth between these two studies, species diversity was likely impacted by the number of raw sequences obtained from each sample. This observation, paired with the large levels of environmental and background DNA contamination, highlights the difficulties in using alpha-diversity metrics to accurately assess diversity in ancient samples.

Differences between samples (beta-diversity) were examined by calculating Bray Curtis distances between all samples within the rarefied (*i.e.* an equal number of sequences or all taxa identified) and complete data sets. Pairwise Bray Curtis distances in MEGAN5 were calculated from the genus level subtree of Bacteria and Archaea. UPGMA trees were built using these distances in SplitsTree and visualized in FigTree. Within the complete data set, the analysis identified four distinct clusters (Figure 2B and Extended Data Figure 9A). Each of the four clusters is described in the main text and can be easily differentiated by the large-scale changes in Gram-positive/negative proportions (Extended Data Figure 9B). The rarefied data revealed similar placement of European samples, but the placement of the African individuals

varied between the two approaches (Extended Data Figure 9A). The rarefied data was limited to only 340 sequences per sample, as some of the African individuals contained few identifiable sequences. Rarefying the data to this level is likely inappropriate and may bias the clustering. For example, the complete data set revealed an increase in support for the identified nodes (*i.e.* nodes values in Figure 2B compared to Extended Data Figure 9A), and samples did not cluster based on sequencing depth when the complete data set was analysed. With the complete data set, the placement of non-African samples remained consistent, suggesting that depth does not contribute to their placement on the tree. Therefore, we chose to compare the differences between each of the four main clusters identified within the complete data set in the main text, utilizing all of the limited taxa identified for the African samples for their placement on the tree.

There are several interesting observations within these four groups. Surprisingly, one LBK individual (Tubingen collection 1979, grave 111) clustered with Mesolithic and Para-Neolithic European hunter-gatherers (6645 +/- 30 BP (Late Mesolithic) to 4690 +/- 40 BP (Para-Neolithic, Zedmar culture)) and the Spy II individual. Misidentification or cultural admixture does not likely explain this observation, as this LBK individual possesses an H mitochondrial DNA haplotype[75], as expected in early European farmers. While speculative, Neandertal and AMH interaction, climatic alterations, or unknown biocultural changes could have all contributed to this observation. Ancient calculus samples from another study by Warinner *et al.*[31] also cluster with the agriculturalist group, as expected, reflecting the robustness of this approach. Despite these differences, the separation of ancestral hunter-gatherers and modern individuals from agriculturalists is clear.

783 Despite these large-scale differences, several species were also shared across
784 multiple samples. For example, 18 different species were conserved across
785 chimpanzees, Neandertals, and modern humans (Table S8), and each contained
786 damage patterns consistent with sample age (Extended Data Figure 7), indicating
787 several oral taxa that have been conserved over evolutionary time. The average DNA
788 damage in these conserved bacterial species was less in the El Sidrón Neandertals
789 (31% C-to-T to 36% G-to-A) than damage observed in the published mitochondrial
790 DNA (mtDNA) sequences from a related individual (El Sidrón 1253 mtDNA; 50% C-
791 to-T)[76] (Extended Data Figure 7A), consistent with previous findings[77]. Surprisingly,
792 apparent damage in Spy bacterial species was markedly less (0.04-13% C-to-T and
793 11-12% G-to-A) but was still demonstrably higher than that from modern specimen
794 (3% for both C-to-T and G-to-A). As mapped read lengths in Spy Neandertals were
795 not indicative of modern cross contamination (54 bp) (Extended Data Figure 7B),
796 inefficient mapping in these species could contribute this phenomenon; 89% fewer
797 reads mapped in Spy Neandertals compared to El Sidrón Neandertals due to low
798 library complexity. In comparison, the average read length for bacterial species in El
799 Sidrón Neandertals appeared ancient (50 bp) and was similar to the length of
800 published mtDNA sequences (52 bp). Damage of mitochondrial DNA within ancient
801 calculus could not be assessed, as minimal Neandertal mitochondrial DNA sequences
802 were identified (El Sidrón 1:5; El Sidrón 2:0; Spy 1:56; Spy 2:0; <0.00004% of the
803 total reads), although the identified sequences were longer than expected (~82.3 bp)
804 (Table S13). In contrast, 9.4-fold coverage (99.6%) of a human mitochondrial genome
805 could be reconstructed from modern calculus (1.5% C-to-T damage) (Table S13).
806 Despite studies that have applied hybridization enrichment techniques to obtain
807 mtDNA sequences from historic dental calculus[78], these results suggest that human

DNA is not a substantial component of ancient dental calculus, suggesting that human DNA may be excluded or degrade more rapidly because it is not a structural component of the bacterial biofilm.

Table S8 – Species shared with Neandertals, chimpanzee and modern human samples were identified in MEGAN5 from the MALTX analysis. Percentage of total identified species were calculated and displayed for each sample.

	Chimpanzee	El Sidron 1	El Sidron 2	Spy 1	Spy 2	Modern
Actinobacteria - *Actinomyces naeslundii*	0.22%	2.64%	8.36%	0.34%	0.01%	0.29%
Actinobacteria - *Actinomyces odontolyticus*	0.15%	0.63%	0.91%	0.24%	1.02%	0.11%
Actinobacteria - *Actinomyces sp. ICM47*	0.09%	0.30%	0.37%	0.15%	0.05%	0.01%
Actinobacteria - *Actinomyces sp. oral taxon 178*	0.67%	1.40%	0.57%	0.12%	0.01%	0.66%
Actinobacteria - *Actinomyces sp. oral taxon 849*	1.05%	4.32%	11.47%	0.45%	1.39%	0.26%
Actinobacteria - *Corynebacterium durum*	0.01%	0.06%	0.04%	0.03%	1.27%	0.05%
Bacteroidetes - *Prevotella intermedia*	0.42%	0.38%	0.08%	0.01%	1.23%	0.06%
Firmicutes - *Gemella haemolysans*	0.02%	0.03%	0.25%	0.06%	0.65%	0.07%
Firmicutes - *Streptococcus sanguinis*	0.10%	1.00%	3.78%	1.40%	9.46%	0.08%
Firmicutes - *Mogibacterium sp. CM50*	13.20%	2.74%	3.38%	0.97%	13.88%	0.03%
Firmicutes - *Dorea longicatena*	0.01%	0.04%	0.04%	0.03%	0.12%	0.01%
Firmicutes - *Johnsonella ignava*	0.21%	0.67%	2.69%	0.35%	0.02%	0.47%
Firmicutes - *Lachnoanaerobaculum saburreum*	0.38%	0.19%	0.37%	0.07%	0.06%	0.23%
Firmicutes - *Lachnospiraceae oral taxon 107*	0.15%	0.15%	0.25%	0.03%	0.60%	0.17%
Firmicutes - *Filifactor alocis*	0.33%	0.37%	0.28%	0.07%	0.97%	0.02%
Firmicutes - P*eptostreptococcus anaerobius*	0.02%	0.12%	0.04%	0.03%	1.21%	0.03%
Firmicutes - *Peptostreptococcus stomatis*	0.11%	3.86%	0.77%	0.44%	10.25%	0.52%
Spirochaetes - *Treponema vincentii*	0.27%	0.32%	0.15%	0.04%	0.41%	5.98%

Specific Pathogen Identification and Analysis

Once species-level identifications were obtained using MALTX, specific oral and respiratory pathogens of interest were examined more closely. To ensure authenticity of pathogen identifications, at least four of the following five criteria were required:

1.) Several genes from the pathogen must be identified in sequenced data (i.e. >20 genes identified in MALTX results).
2.) Genome-wide reference-mapping and damage analysis must reveal DNA damage patterns indicative of ancient DNA fragments, *i.e.* >500 reads mapping to a reference genome with C-to-T rates expected for thermal age.
3.) The pathogen cannot be detected in extraction blank control samples or environmental samples (*i.e.* soil) that was analysed using similar methods.
4.) The pathogen of interest cannot be closely related to common commensal oral isolates, *i.e.* its lineage must pertain to a unique branch on a phylogenetic tree.
5.) Skeletal or paleopathological evidence should exist within the population to support the existence of the disease caused by the pathogen.

Each of the pathogens identified within this study (Tables S9 and S10) were scrutinized using these criteria. These criteria provide a conservative guideline for pathogen identification but cannot differentiate between progenitor strains and current pathogenic strains in ancient samples. In the case of several pathogens identified in ancient samples, their identifications may be attributed to progenitor or closely related ancestral strains of modern day pathogens. This method is also unable to accurately predict if individuals suffered from the disease or simply carried the pathogen asymptomatically.

Several modern pathogens were identified in ancient samples, but were also identified in environmental control samples (Table S9 and S10). The caries-associated pathogen *Streptococcus mutans* was identified in all Neandertals (0.08% to 0.18%), as well as fresh ground water. All three members of the 'red complex' pathogens associated with periodontal disease were identified in Neandertals (*Porphyromonas gingivalis*: 0-0.52%; *Tannerella forsythia* 0.05-2.4%; and *Treponema denticola* 0-1.87%) and fresh ground water (Table S9). It is unlikely that these obligate human pathogens from the oral cavity can survive in the environment, so we examined if these oral species were present in common laboratory reagents. *T. denticola, P. gingivalis,* and *T. forsythia* were all identified in a common DNA extraction kit (Table S9). While environmental samples were extracted using kits, the ancient samples in this study were extracted using homemade QG silica method that is free of these pathogens, as demonstrated by the EBCs extracted simultaneously with ancient samples (QG EBCs 1-2) (Table S9). Further, DNA from these pathogens in Neandertals contained damage indicative of ancient DNA (Table S11). Together, these data indicates that Neandertals shared these pathogens, or at least ancestral forms or genetic content of these pathogens, with modern humans.

This approach also identified five nasopharyngeal and respiratory pathogens in Neandertals that were absent in all controls and environmental samples: *Bordetella parapertussis* (whooping cough), *Pasteurella multocida* (skin and respiratory infections), *Streptococcus pyogenes* (strep throat), *Corynebacterium diptheriae* (diphtheria), and *Neisseria gonorrhoeae* (gonorrhoea) (Table S9). In El Sidrón samples, each of these pathogens contained DNA damage indicative of ancient DNA (Table S12). The first four of these are important nasopharyngeal and respiratory pathogens of modern humans, but *N. gonorrhoeae* does not typically infect the oral

862 cavity. Several of these pathogens (*N. gonorrhoeae*, *S. pyogenes*, and *C. diptheriae*)
863 are also closely related to common oral microorganisms, which confounds accurate
864 identifications in ancient metagenomic samples and therefore disqualifies them from
865 further identification using our methods. For example, genomic mapping and
866 phylogenetic analysis of reads identified to *N. gonorrhoeae* in El Sidrón 2 placed this
867 strain within known commensal oral *Neisseria* isolates (Extended Data Figure 10A).
868 Small fragment size typical of ancient DNA confounds accurate mapping of reads to
869 species and would also likely influence accurate functional profiling. Until enhanced
870 mapping algorithms specific to short ancient DNA molecules are developed for
871 metagenomic analysis, these types of analyses will remain difficult.
872

Table S9 – Identification of Neandertal bacterial pathogens. Species identifications from MALTX analysis were screened for known human bacterial pathogens. The number of confirmed hits to each species is given for all deeply sequenced metagenomes (chimpanzee, Neandertals, and modern human), other published ancient oral metagenomes (WarB61 and G12), extraction blank control (EBC) samples from DNA extraction kits and homemade DNA QG extraction methods, and environmental samples (soil and water). * indicates that the bacterial species is closely related to several common oral species.

Pathogens	Dental Calculus								Extraction Blank Controls			Environmental Samples			
Pathogens in Ancient Dental Calculus	**Chimp**	**El Sidron 1**	**El Sidron 2**	**Spy 1**	**Spy 2**	**War B61**	**War G12**	**Modern**	**Kit EBC**	**QG EBC 1**	**QG EBC 2**	**Bracc. Water**	**Grnd Water**	**GrssInd Soil**	**Forest Soil**
Bordetella parapertussis	0	23	60	24	0	13	0	0	0	0	0	0	0	0	0
Pasteurella multocida	0	20	0	13	0	41	36	0	0	0	0	0	0	0	0
*Neisseria gonorrhoeae**	0	0	116	41	90	58	180	162	0	0	0	0	0	0	0
*Streptococcus pyogenes**	0	37	273	14	0	0	13	0	0	0	0	0	0	0	0
*Corynebacterium diphtheriae**	82	54	90	60	0	70	68	221	0	0	0	0	0	0	0
Pathogens in DNA Extraction Kit Reagents															
Treponema denticola	1506	2826	4502	81	0	2984	10454	6618	8	0	0	24	222	0	21
Porphyromonas gingivalis	15982	785	652	70	0	379	2230	1263	5	0	0	23	277	0	0
Tannerella forsythia	25634	3113	7359	67	342	9286	13605	27860	22	0	0	46	348	0	29
Salmonella enterica	0	29	38	214	0	26	14	0	69	0	0	75	191	131	50
Clostridium botulinum	107	184	236	89	0	83	70	170	1	0	0	52	557	0	40
Pathogens in Environmental Samples															
Streptococcus mutans	18	194	550	95	23	158	133	126	0	0	0	0	55	1388	0
Staphylococcus aureus	0	59	207	102	0	40	28	80	0	0	0	132	186	0	31
Clostridium tetani	0	48	44	0	0	19	17	0	0	0	0	0	84	0	0
Neisseria meningitidis	0	84	472	76	0	175	302	2073	0	0	0	18	84	0	22
Helicobacter pylori	0	70	91	434	483	24	33	93	0	0	0	52	162	0	47
Edwardsiella tarda	0	0	58	12	0	0	0	0	0	0	0	19	0	0	0
Klebsiella pneumoniae	0	14	0	421	0	12	11	204	0	0	0	27	235	0	28
Serratia marcescens	0	0	104	10	0	14	15	0	0	0	0	14	74	0	28
Yersinia pestis	0	0	0	18	0	0	0	0	0	0	0	15	0	0	0
Legionella pneumophila	0	34	112	112	0	0	0	0	0	0	0	273	879	0	220
Pseudomonas aeruginosa	0	28	52	164	0	22	14	75	0	0	0	93	4185	132	81
Vibrio cholerae	0	67	99	92	0	23	17	102	0	0	0	215	603	128	81
Listeria monocytogenes	29	25	80	15	0	19	13	0	0	0	0	0	86	0	0
Campylobacter jejuni	72	57	61	0	0	8	23	116	0	0	0	43	141	0	16
Escherichia coli	94	156	379	647	3	62	37	180	0	0	0	149	562	139	116
Mycobacterium tuberculosis	166	97	159	109	0	13	13	152	0	0	0	547	779	721	646
Fusobacterium nucleatum	3941	675	2022	36	0	116	3950	79947	0	0	0	27	105	0	0

873

874

Table S10 – Identification of common oral pathogens in dental calculus, as well as extraction blank control (EBC) samples and environmental controls. The number of reads identified by MALTX and the percentage of the total reads identified are given, alongside the factor increase of these reads in Neandertals over either the deeply sequenced kit EBC (EBC1) or fresh ground water.

	Porphyromonas gingivalis				*Tannerella forsythia*				*Treponema denticola*				*Streptococcus mutans*			
	Reads Identified	% Identified	Fct Inc over GW	Fct Inc over EBC	Reads Identified	% Identified	Fct Inc over Ground Water	Fct Inc over EBC	Reads Identified	% Identified	Fct Inc over Ground Water	Fct Inc over EBC	Reads Identified	% Identified	Fct Inc over Ground Water	Fct Inc over EBC
Chimpanzee	15982	0.08555%	57.69663	3196.403428	25634	0.13722%	73.66099	1165.178319	1506	0.00806%	6.78380	188.250114	**18**	**9.6357E-07**	**0.327272856**	na
El Sidron 1	785	0.00420%	2.83393	157.0001684	3113	0.01666%	8.94541	141.4995751	2826	0.01513%	12.72976	353.2502139	194	1.03851E-05	3.527274115	na
El Sidron 2	652	0.00349%	2.35379	130.4001399	7359	0.03939%	21.14657	334.4989954	4502	0.02410%	20.27933	562.7503408	550	2.94424E-05	10.00000393	na
Spy 1	70	0.00037%	0.25271	14.00001502	67	0.00036%	0.19253	3.045445399	81	0.00043%	0.36487	10.12500613	95	5.08551E-06	1.727273407	na
Spy 2	0	0.00000%	0.00000	0	342	0.00183%	0.98276	15.54540786	0	0.00000%	0.00000	0	23	1.23123E-06	0.418181988	na
Warinner B61	379	0.00203%	1.36823	75.80008813	9286	0.04971%	26.68393	422.0896415	2984	0.01597%	13.44147	373.0002259	158	8.458E-06	2.872728403	na
Warinner G12	2230	0.01194%	8.05052	446.0004784	13605	0.07283%	39.09486	618.4072337	10454	0.05596%	47.09020	1306.750791	133	7.11971E-06	2.418182769	na
Modern	1263	0.00676%	4.55956	252.6002709	27860	0.14914%	80.05754	1266.359833	6618	0.03543%	29.81088	827.2505011	126	6.74498E-06	2.290909992	na
EBC 1 (Kit)	5	0.00003%	0.01805	1.000001073	22	0.00012%	0.06322	0.999996997	8	0.00004%	0.03604	1.000000606	0	0	0	na
EBC 2 (QG)	0	0.00000%	0.00000	0	0	0.00000%	0.00000	0	0	0.00000%	0.00000	0	0	0	0	na
EBC 3 (QG)	0	0.00000%	0.00000	0	0	0.00000%	0.00000	0	0	0.00000%	0.00000	0	0	0	0	na
Brackish Water	23	0.00012%	0.08303	4.800004934	46	0.00025%	0.13218	2.090902812	24	0.00013%	0.10811	3.000001817	0	0	0	na
Ground Water	277	0.00148%	1.00000	55.40005942	348	0.00186%	1.00000	15.81813431	222	0.00119%	1.00000	27.7500168	55	2.94424E-06	1.000000393	na
Grassland Soil	0	0.00000%	0.00000	0	0	0.00000%	0.00000	0	0	0.00000%	0.00000	0	1388	7.43019E-05	25.23637356	na
Forest Soil	0	0.00000%	0.00000	0	29	0.00016%	0.08333	1.318177859	21	0.00011%	0.09459	2.625000159	0	0	0	na

875
876

Table S11 – MapDamage analysis was performed on the reads mapping to oral bacterial pathogen genomes in chimpanzee, Neandertal, and modern human specimens.

Ancient Library	Reference	All Mapped Reads	Mapped Reads >Q30	Deduplicted Mapped Reads	5' C-T Proportion	3' G-A Proportion	Increase Purines Before Start	Decrease Pyrimindines Before Start	Average Length	St Dev Length	Cytosine Deamination in Dbl Strds (DeltaD)	Cytosine Deamination in Single Strds (DeltaS)	Avg Length of Single Strd Overhangs (Lambda)	Ratio of DeltaD to DeltaS
DCCHIMP	NC002967TreponemadenticolaATCC35405	9353	2640	177	0	0.04	0.62	3.04	32.66	13.67	0.03	0.29	0.7	0.103448
DCELSIDRON1	NC002967TreponemadenticolaATCC35405	30753	18556	11596	0.38	0.44	1.57	0.53	52.66	13.12	0.02	1	0.34	0.02
DCELSIDRON2	NC002967TreponemadenticolaATCC35405	32689	20390	1978	0.33	0.39	1.63	0.53	57.16	21.01	0.03	0.98	0.39	0.030612
DCSPYNEW	NC002967TreponemadenticolaATCC35405	437	2	2	0	0	0.5		36.5	9.19	0.1	0.47	0.56	0.212766
DCSPYOLD	NC002967TreponemadenticolaATCC35405	1341	111	75	0	0.08	0.96	1.07	36.96	21.1	0.04	0.32	0.65	0.125
DCMODERN	NC002967TreponemadenticolaATCC35405	19351	7942	7572	0.03	0.02	0.89	1.13	59.94	25.57	0.03	0.15	0.71	0.2
DCCHIMP	NC004350StreptococcusmutansUA159	9554	412	62	0	0	0.59	3.75	26.84	5.1	0.09	0.39	0.51	0.230769
DCELSIDRON1	NC004350StreptococcusmutansUA159	17931	1026	617	0.25	0.26	1.49	0.6	46.28	12.2	0.01	0.9	0.45	0.011111
DCELSIDRON2	NC004350StreptococcusmutansUA159	31849	2676	259	0.26	0.25	1.32	0.68	46	15.01	0	0.83	0.5	0
DCSPYNEW	NC004350StreptococcusmutansUA159	4420	440	9	0	0	5	0.5	39.89	9.03	0.05	0.41	0.59	0.121951
DCSPYOLD	NC004350StreptococcusmutansUA159	3778	368	128	0.11	0	1.42	0.55	49.38	19.86	0.01	0.34	0.74	0.029412
DCMODERN	NC004350StreptococcusmutansUA159	19696	1472	1391	0.02	0.03	0.89	1.12	46.45	19.62	0.01	0.23	0.79	0.043478
DCCHIMP	NC010729PorphyromonasgingivalisATCC33277	126008	100828	2350	0.02	0.01	0.87	1.21	46.17	19.56	0.03	0.09	0.56	0.333333
DCELSIDRON1	NC010729PorphyromonasgingivalisATCC33277	22238	12985	7493	0.44	0.51	1.61	0.52	50.04	12.51	0	1	0.33	0
DCELSIDRON2	NC010729PorphyromonasgingivalisATCC33277	18765	7547	720	0.42	0.35	1.62	0.57	48.19	16.68	0.01	0.97	0.36	0.010309
DCSPYNEW	NC010729PorphyromonasgingivalisATCC33277	175	7	6	0	0	3	0.6	38.33	21.13	0.04	0.44	0.59	0.090909
DCSPYOLD	NC010729PorphyromonasgingivalisATCC33277	2348	145	63	0	0.08	0.84	1.23	51.17	29.4	0.01	0.37	0.75	0.027027
DCMODERN	NC010729PorphyromonasgingivalisATCC33277	42018	13938	13153	0.02	0.02	0.84	1.17	60.93	26.04	0.01	0.12	0.69	0.083333
DCCHIMP	NC016610TannerellaforsythiaATCC43037	220888	166503	4325	0.02	0.01	0.81	1.35	43.68	17.93	0.03	0.01	0.47	3
DCELSIDRON1	NC016610TannerellaforsythiaATCC43037	71435	50388	30085	0.42	0.46	1.63	0.5	49.21	11.84	0.01	1	0.34	0.01
DCELSIDRON2	NC016610TannerellaforsythiaATCC43037	94682	66842	6209	0.41	0.42	1.62	0.53	49.23	15.8	0.01	1	0.34	0.01
DCSPYNEW	NC016610TannerellaforsythiaATCC43037	181	8	8	0.33	0	1.2	0.67	41.25	16.14	0.04	0.58	0.49	0.068966
DCSPYOLD	NC016610TannerellaforsythiaATCC43037	2671	347	152	0.09	0.12	1	1	45.25	19.59	0.01	0.44	0.54	0.022727
DCMODERN	NC016610TannerellaforsythiaATCC43037	131223	98558	93666	0.01	0.01	0.84	1.17	64.97	27.22	0.01	0.07	0.57	0.142857

877
878

Table S12 – MapDamage analysis was performed on the reads mapping to pathogenic bacterial genomes in chimpanzee, Neandertal, and modern human specimens.

Ancient Library	Reference	All Mapped Reads	Mapped Reads >Q30	Deduplicted Mapped Reads	5' C-T Proportion	3' G-A Proportion	Increase Purines Before Start	Decrease Pyrimindines Before Start	Average Length	St Dev Length	Cytosine Deamination in Dbl Strds (DeltaD)	Cytosine Deamination in Single Strds (DeltaS)	Avg Length of Single Strd Overhangs (Lambda)	Ratio of DeltaD to DeltaS
DCCHIMP	NC009567HaemophilusinfluenzaePittGG	6645	387	43	0	0	0.64	2.86	26.67	3.85	0.06	0.32	0.64	0.1875
DCELSIDRON1	NC009567HaemophilusinfluenzaePittGG	11510	477	319	0.18	0.46	1.68	0.49	44.49	11.21	0.01	0.9	0.45	0.011111
DCELSIDRON2	NC009567HaemophilusinfluenzaePittGG	18201	997	127	0.47	0.32	1.5	0.61	41.23	12.63	0.02	0.84	0.46	0.02381
DCSPYNEW	NC009567HaemophilusinfluenzaePittGG	1591	523	5	0	0	0.75	2	39.2	13.72	0.03	0.42	0.65	0.071429
DCSPYOLD	NC009567HaemophilusinfluenzaePittGG	3124	220	90	0	0.05	0.83	1.32	56.7	30.77	0.01	0.33	0.78	0.030303
DCMODERN	NC009567HaemophilusinfluenzaePittGG	15518	1545	1469	0.03	0.03	0.84	1.2	53.21	24.2	0.03	0.16	0.67	0.1875
DCCHIMP	NC010120Neisseriameningitidis053442	6850	839	122	0.03	0.03	0.88	1.19	27.28	5.25	0	0.28	0.78	0
DCELSIDRON1	NC010120Neisseriameningitidis053442	13536	1459	995	0.29	0.33	1.57	0.53	44.82	12.85	0	0.96	0.45	0
DCELSIDRON2	NC010120Neisseriameningitidis053442	40893	9157	1227	0.28	0.32	1.72	0.49	47.39	16.59	0	0.96	0.42	0
DCSPYNEW	NC010120Neisseriameningitidis053442	3154	1761	12	0	0	1.67	0.33	45.67	12.67	0.03	0.35	0.66	0.085714
DCSPYOLD	NC010120Neisseriameningitidis053442	3394	341	163	0.2	0.07	1.01	0.99	49.77	23.22	0	0.62	0.74	0
DCMODERN	NC010120Neisseriameningitidis053442	81524	36252	34435	0.03	0.03	0.82	1.2	58.18	23.67	0	0.16	0.91	0
DCCHIMP	NC016802CorynebacteriumdiphtheriaeHC02	13435	1131	118	0	0.02	0.88	1.23	29.37	6.28	0	0.25	0.79	0
DCELSIDRON1	NC016802CorynebacteriumdiphtheriaeHC02	32098	1970	1275	0.17	0.26	1.63	0.53	45.47	13.66	0	0.95	0.59	0
DCELSIDRON2	NC016802CorynebacteriumdiphtheriaeHC02	34010	1106	241	0.18	0.15	1.35	0.63	36.17	12.15	0	0.74	0.67	0
DCSPYNEW	NC016802CorynebacteriumdiphtheriaeHC02	2278	38	4	0	0	0.67	2	37	14.24	0.07	0.4	0.61	0.175
DCSPYOLD	NC016802CorynebacteriumdiphtheriaeHC02	3882	385	169	0.03	0.06	0.93	1.13	56.44	27.67	0	0.36	0.82	0
DCMODERN	NC016802CorynebacteriumdiphtheriaeHC02	35074	4729	4387	0.03	0.03	0.8	1.27	47.49	16.45	0	0.2	0.85	0
DCCHIMP	NZJLCX00000000MycobacteriumtuberculosisT85	18229	11345	712	0.02	0.01	1.07	0.92	32.64	12.04	0	0.18	0.87	0
DCELSIDRON1	NZJLCX00000000MycobacteriumtuberculosisT85	36572	23674	12507	0.32	0.38	1.57	0.54	49.94	13.68	0	1	0.49	0
DCELSIDRON2	NZJLCX00000000MycobacteriumtuberculosisT85	39687	25850	2997	0.33	0.31	1.66	0.51	48.24	16.74	0	0.99	0.49	0
DCSPYNEW	NZJLCX00000000MycobacteriumtuberculosisT85	2380	1284	21	0.29	0.38	1.36	0.6	49.1	14.98	0.02	0.72	0.53	0.027778
DCSPYOLD	NZJLCX00000000MycobacteriumtuberculosisT85	4086	2566	1014	0.15	0.1	1.17	0.79	54.3	19.81	0	0.96	0.67	0
DCMODERN	NZJLCX00000000MycobacteriumtuberculosisT85	21312	14822	12933	0.04	0.04	0.84	1.19	54.24	20.08	0	0.21	0.88	0
DCCHIMP	NC018828BordetellaparapertussisBpp5	11236	2630	482	0.02	0.01	0.91	1.11	26.5	2.94	0	0.2	0.87	0
DCELSIDRON1	NC018828BordetellaparapertussisBpp5	16927	2409	1677	0.2	0.19	1.47	0.61	41.18	12.64	0	0.95	0.65	0
DCELSIDRON2	NC018828BordetellaparapertussisBpp5	40694	5507	1073	0.21	0.21	1.47	0.63	39.6	13.43	0	0.93	0.63	0
DCSPYNEW	NC018828BordetellaparapertussisBpp5	2055	781	18	0	0	1	1	32.94	8.39	0.02	0.35	0.7	0.057143
DCSPYOLD	NC018828BordetellaparapertussisBpp5	4516	703	373	0.05	0.02	0.84	1.26	42.26	18.34	0	0.79	0.79	0
DCMODERN	NC018828BordetellaparapertussisBpp5	28863	6944	6614	0.03	0.02	0.78	1.27	57.77	28.46	0	0.15	0.92	0

879
880

Table S13 – MapDamage analysis was performed on the reads mapping an ancient Neandertal mitochondrial genome (1253). The number of reads mapping to each species reference genome at a quality threshold of Q30 and unduplicated is shown, along with the percentage of damage associated mutations and average read length.

Ancient Library	Reference	All Mapped Reads	Mapped Reads >Q30	Deduplicted Mapped Reads	5' C-T Proportion	3' G-A Proportion	Increase Purines Before Start	Decrease Pyrimindines Before Start	Average Length	St Dev Length	Cytosine Deamination in Dbl Strds (DeltaD)	Cytosine Deamination in Single Strds (DeltaS)	Avg Length of Single Strd Overhangs (Lambda)	Ratio of DeltaD to DeltaS	Total Reads	Percent Total Reads
DCCHIMP	ElSidron1253mtDNAgenome	12	8	1	0	0	0		36		0.14	0.46	0.54	0.304	17575167	0.00007
DCELSIDRON1	ElSidron1253mtDNAgenome	14	14	5	0	0	0.5	3	82.2	22.64	0.07	0.48	0.55	0.146	50238935	0.00003
DCELSIDRON2	ElSidron1253mtDNAgenome	0	0	0	0	0				0	0.5	0.49	0.5	1.020	48231792	0.00000
DCSPYNEW	ElSidron1253mtDNAgenome	0	0	0	0	0				0	0.5	0.5	0.51	1.000	17604340	0.00000
DCSPYOLD	ElSidron1253mtDNAgenome	185	180	56	0.18	0	0.94	1.08	82.36	25.02	0.01	0.41	0.77	0.024	13530309	0.00137
DCMODERN	ElSidron1253mtDNAgenome	2430	2397	2259	0.02	0.01	0.86	1.16	67.4	27.79	0.01	0.19	0.78	0.053	29466684	0.00825

881
882

883 The application of authenticity criteria did suggest that *Bordetella*
884 *parapertussis*, a bacterial respiratory pathogen that causes whooping cough, and
885 *Pasteurella multocida*[79], a bacterial pathogen known to cause lethal co-infections with
886 whooping cough, in the El Sidrón Neandertals (Table S9) may be endogenous. In both
887 specimens, the *Bordetella* reads mapped most closely to a zoonotic isolate of *B.*
888 *parapertussis* strain BPP5 and included bordetellae specific genes (*i.e.* BPP5 fosmid
889 and filamentous hemagglutinin encoding genes, *fha*). Reads mapping to the BPP5
890 genome from both Neandertals were ancestral to all pathogenic classical bordetellae,
891 including zoonotic isolates of *Bordetella bronchiseptica* and human-restricted strains
892 of *Bordetella pertussis* (Extended Data Figure 10B). Currently, there are no known or
893 closely related human oral isolates of *Bordetella* or *Pasteurella*, and phylogenetic
894 analysis identified *B. parapertussis* reads as basal to many modern *Bordetella*
895 pathogens. Despite adhering to these criteria, the observation of *B. paraperutssis* in El
896 Sidrón Neandertals could be explained by either the presence of an ancestral form of
897 *Bordetella*, *B. bronchiseptica* present within soil at the site, or more simply by noise
898 and inefficient mapping in the data set. To test the efficiency of the mapping, we
899 directly compared mapping quality scores from reads that mapped to two genomes
900 (Table S14), identifying which reads mapped more efficiently to a specific genome.
901 Only 20% of reads that mapped to *B. parapertussis* more efficiently mapped to *B.*
902 *petrii*, and even fewer reads more efficiently mapped to *B. parapertussis* than to a
903 highly unrelated *Neisseria* pathogen, confounding the accurate identification of *B.*
904 *parapertussis* in Neandertals. Further analysis and the development of more accurate
905 mapping tools that handle short reads will be required to accurately identify this
906 pathogen. Nevertheless, the identification of oral pathogens and *Bordetella* within
907 Neandertals may indicate that these pathogens have been evolving with hominins over

908 expansive time periods and did not originate during a recent zoonotic episode during
909 animal domestication[80].
910

Table S14 – Mapped reads against a variety of genomes (*B. parapertussis*, *B. petrii*, *Neisseria gonorrhea*, and *Streptococcus oralis*) were compared using a script developed to compare the mapping quality scores of reads identified in two datasets to be compared directly. 'Okay' refers the number of reads that more accurate map to the first test genome (*i.e.* the genome of interest), while 'NonInf' refers to the reads that are non informative, *i.e.* do not map better to either genome. 'Contam' sequences are those that map better to the contaminant genome, *i.e.* the second genome in the test.

Sample	Read Length	Test	Okay	NonInf	Contam	Error	Proportion Bpp
ELSIDRON1	30	Bpp vs Bpet	188	0	681	0	0.216340621
ELSIDRON1	25	Bpp vs Bpet	224	0	951	0	0.190638298
ELSIDRON1	25	Bpp vs Ngon	15	0	1075	0	0.013761468
ELSIDRON1	25	Bpp vs Strep	1	0	6510	0	0.000153586

While Neandertals went extinct >30,000 years prior to the onset of agriculture, their pathogens provide critical information to examine the history and origin of infections in modern humans. The Neolithic Revolution, with large dietary shifts, domestication of animals, sedentary lifestyles, and decreased sanitation[81], is estimated to be the single most important event to impact human disease[82] and is believed to be a significant driver of pathogen evolution[83]. However, the identification of a whooping cough and several other conserved oral and respiratory bacterial pathogens within Neandertals indicates that several infectious diseases, thought to have been first transmitted after the onset of agriculture, existed in hominids well before this transition. Hence, modern 'zoonotic' pathogens may not have been introduced into humans during domestication and are potentially the result of genomic evolution or different selection pressures that arose during the Neolithic Revolution. This also suggests that these pathogens, or at least their ancestral forms, have been shared over longer evolutionary time spans than previously estimated. Further studies aimed at examining the genomic evolution through time in pathogens will likely uncover molecular mechanisms of evolution responsible for the spread of infectious agents during the Neolithic Revolution.

Methanobrevibacter Analysis

Oral *Methanobrevibacter* taxa are very similar to *Methanobrevibacter* species found in the gut (*i.e. M. smithii*) and differ largely through the loss of several large adhesion associated genes likely used to attach to the epithelial cells of the intestinal tract. Therefore, we wanted to investigate the evolutionary history of *M. oralis* subsp. *neandertalensis* further to (1) identify if archaeal DNA degrades at a rate similar to bacterial DNA, (2) reveal if there were similarities to the archaeal gut relative, and (3) determine when the oral and the gut *Methanobrevibacter* taxa diverged. First, we

mapped ancient sequences to *M. smithii* and to *M. oralis*. 79% fewer genes mapped to *M. smithii* ATCC 35061 than mapped to *M. oralis* JMR01 genome, and the ancient strain also lacked genes for adhesion in the gastrointestinal tract. This suggests that the strain in the oral cavity of El Sidrón 1 is indeed *M. oralis*. Maximum likelihood phylogenetic analysis with RAxML also confirmed this, as *M. oralis* subsp. *neandertalensis* was more similar to *M. oralis* JMR01 than a wide-range of *M. smithii strains*. The damage patterns were also consistent for a bacterial species of similar age (Table 2). We also found that the rate of degradation in Gram-positive (*Peptostreptococcus stomatis*; 54.6 bp; 36% C-to-T; 40% G-to-A), Gram-negative (*Propionibacterium propionicu*m; 48.8 bp; 37% C-to-T; 43% G-to-A), and eubacterial taxa (*Eubacterium sphenum*; 52.8 bp; 37% C-to-T; 41% G-to-A) was similar to that observed in archaea (*Methanobrevibacter oralis*; 58.67; 33% C-to-T; 36% G-to-A), suggesting that cell wall structure does not play a role in bacterial DNA preservation over long time periods. The damage observed in *M. oralis* was also lower than previously observed in the mitochondrial DNA from a contemporaneous El Sidron Neandertal (El Sidron 1253 mtDNA; 50% C-to-T; 52 bp)[76], as has been previously observed with bacteria[84].

Using a tip-dated ancient genome, we wanted to examine both when oral archaeal taxa diverged from related gut strains and when the Neandertal and human *M. oralis* strains diverged. In addition to comparative genomic analysis (Table S15), we found poor mixing of the Markov chain in BEAST for our analyses of two *M. oralis*, four *M. smithii*, and one *Methanobrevibacter wolinii* (an outgroup) strains under the uncorrelated lognormal relaxed clock model. We attributed this to the fact that our data set consists of a small number of taxa (*i.e.* this clock model is over parameterised). In particular, every branch in the tree can have a different rate under

this model. These rates are described using two parameters: the mean rate across branches and the standard deviation of the branch rates, both of which may be difficult to calculate for phylogenetic trees with few taxa (*i.e.* less than 20 branches). Therefore, we interpreted the estimates from the strict clock model. Previous studies involving dated tips have suggested that the mean estimates from this model are generally comparable to those from relaxed clock model[85]. To verify that these estimates were not mislead by high rate variation, we also conducted our analyses in BEAST after selecting a subset of 192 genes with the smallest departure from clocklike behaviour according to their coefficient of rate variation. We assessed the impact of high rate variation among lineages in our estimates by repeating our analyses in BEAST with these 192 genes with the strongest clocklike behaviour, and the analysis produced largely congruent estimates of evolutionary rates and divergence times. Therefore, a strict clock was utilized to estimate dates provided in this study. While the date estimate for the Neandertal and human *M. oralis* strains is discussed in the main text, the data for the split between *M. oralis* and *M. smithii* was observed to be 832 kyr (95% highest posterior density interval 715K-971 kyr; Figure 3B). This directly precedes the split of Neandertals and early anatomically modern humans, assuming this split occurred as early as 700,000 years ago as molecular dating currently suggests[86].

Table S15 – Coding DNA sequences (CDS) that were missing in *M. oralis neandertalensis* but present in *M. oralis* in modern humans are displayed, only if the function was known. 81 genes missing in *M. oralis neandertalensis* were annotated as hypothetical proteins and are not displayed.

Name	Minimum	Maximum	Length	Direction
2-C-methyl-D-erythritol 4-phosphate cytidylyltransferase CDS	144007	144702	696	reverse
2,5-diketo-D-gluconic acid reductase CDS	24887	25720	834	forward
2,5-diketo-D-gluconic acid reductase CDS	26333	27230	898	forward
3-phosphoshikimate 1-carboxyvinyltransferase CDS	348407	349723	1317	reverse
7-cyano-7-deazaguanine synthase CDS	146022	146696	675	forward
ABC transporter CDS	2247	3892	1646	reverse
ABC transporter CDS	213147	213917	771	reverse
ABC transporter CDS	22560	24290	1731	reverse
acetyltransferase CDS	217914	218720	807	forward
alpha/beta hydrolase CDS	15018	15992	975	reverse
ammonia channel protein CDS	<324463	325557	>1095	reverse
appr-1-p processing enzyme family domain-containing protein CDS	421943	422725	783	reverse
asparagine synthetase CDS	274918	276366	1449	reverse
ATPase CDS	95405	96640	1236	reverse
ATPase CDS	99167	100366	1200	reverse
ATPase CDS	27818	29050	1233	reverse
cation transporter CDS	182373	184227	1855	forward
cation transporter CDS	16062	18081	2020	reverse
CRISPR-associated endonuclease Cas2 CDS	27409	27675	267	reverse
CRISPR-associated endoribonuclease Cas6 CDS	124963	125703	741	reverse
CRISPR-associated protein CDS	18877	20124	1248	reverse
cupin CDS	25795	26226	432	forward
cysteine desulfurase CDS	341274	342458	1185	reverse
cysteine synthase CDS	346747	347693	947	reverse
DNA methyltransferase CDS	117589	119136	1548	forward
DNA mismatch repair protein MutT CDS	265100	265504	405	forward
DUF2634 domain-containing protein CDS	71266	71694	429	reverse
endonuclease III CDS	347784	348407	624	reverse
formate dehydrogenase family accessory protein FdhD CDS	393696	394460	765	forward
glycerol-3-phosphate dehydrogenase CDS	144712	145680	969	reverse
GshA CDS	167178	168571	1394	forward
HNH endonuclease CDS	97246	97863	618	reverse
integrase CDS	110585	111695	1111	reverse
iron-sulfur cluster assembly scaffold protein NifU CDS	340890	341261	372	reverse
KlaA protein CDS	52163	53302	1140	reverse
KTSC domain-containing protein CDS	101752	101964	213	forward
MATE family efflux transporter CDS	263908	265272	1365	reverse
membrane protein CDS	90942	91751	810	forward
methyltransferase CDS	350273	351055	783	reverse
nitrogen regulatory protein P-II 1 CDS	323223	323561	339	reverse
NrdH-redoxin CDS	27815	28096	282	forward
NUDIX domain-containing protein CDS	146181	146597	417	forward
phosphate ABC transporter ATPase CDS	211638	212692	1055	reverse
phosphatidate cytidylyltransferase CDS	410238	410912	675	reverse
PIN domain-containing protein CDS	126213	126602	390	forward
pyridoxamine 5'-phosphate oxidase CDS	18405	18806	402	reverse
QacE family quaternary ammonium compound efflux SMR transporter CDS	145813	146133	321	forward
restriction endonuclease CDS	190474	190989	516	reverse
restriction endonuclease CDS	105010	106892	1883	forward
SAM-dependent methyltransferase CDS	217129	217911	783	forward
SAM-dependent methyltransferase CDS	220837	221415	579	forward
Sir2 silent information regulator family NAD-dependent deacetylase CDS	421093	421941	849	reverse
sugar fermentation stimulation protein CDS	447396	448158	763	forward
type I restriction endonuclease CDS	114455	117580	3126	forward

983 **16S rRNA amplicon comparisons to shotgun sequencing**

984 Rapid and inexpensive amplicon sequencing has been applied to ancient
985 metagenomes[1,31], despite the fact that amplicon libraries are biased by amplicon
986 selection, construction, and fragment length (reviewed in [87]). As a result of DNA
987 breakdown over time (taphonomy), ancient amplicon libraries may suffer from
988 additional bias introduced from short DNA fragment lengths. To determine the
989 efficacy of 16S rRNA amplicon sequencing on ancient samples, the 16S rRNA and
990 shotgun sequencing (>10 million reads per sample) data sets were compared for five
991 samples: chimpanzee, El Sidrón 1, El Sidrón 2, Spy 1, Spy 2, and modern human
992 C10. We first compared the 16S rRNA amplicon libraries to shotgun metagenomes
993 constructed from the same ancient and modern samples (Figure 1; Extended Data
994 Figure 1). This revealed drastically different microbial community structures between
995 the two approaches (Table S16). Differences between the samples were not limited to
996 specific bacterial phyla (Extended Data Figure 1), as Gram-positive, Gram-negative,
997 and archaeal phyla were all impacted (Table S16) despite different outer cell wall
998 structures. In fact, UPGMA clustering of Euclidean distances revealed that in most
999 cases filtered and unfiltered ancient 16S rRNA libraries were more similar to
1000 themselves than to the shotgun data produced from their respective samples (Figure
1001 1). In contrast, data sets generated from a modern specimen clustered together and
1002 were not subject to the same level of bias observed in ancient samples (Figure 1;
1003 Extended Data Figure 1). There are two key issues that likely contribute to this.
1004

Table S16 – Filtered 16S amplicon datasets were compared to filtered shotgun datasets at the phyla level, and the proportion differences between the two datasets are shown. Values >5% are highlighted in red.

Proportion differences in filtered shotgun vs 16S rRNA data sets	Chimpanzee	El Sidron 1	El Sidron 2	Spy 1	Spy 2	Modern
Bacteria; Fusobacteria	501.41	0.16	1.52	0.01	0.00	0.31
Bacteria; Bacteroidetes	7.81	0.40	0.94	5.48	0.49	3.01
Bacteria; Actinobacteri	4.93	7.37	0.82	1.45	1.18	1.81
Bacteria; Proteobacteria	1.33	0.23	0.62	0.68	0.24	1.25
Bacteria; Synergistetes	1.15	0.99	5.47	0.01	0.00	0.32
Archaea; Euryarchaeota	0.86	10.16	17.04	0.55	53.17	1.22
Bacteria; Firmicutes	0.38	3.02	33.71	0.85	157.96	0.46
Bacteria; Chloroflexi	0.02	0.63	1.96	0.12	0.01	0.30
Bacteria; Cyanobacteria	0.01	0.00	0.00	0.00	20.14	0.00
Bacteria; Acidobacteria	0.00	0.01	0.00	0.06	0.00	0.00
Bacteria; Planctomycetes	0.00	0.00	0.00	0.06	1.14	0.00
Bacteria; Spirochaetes	0.00	1.58	9.25	0.00	0.00	3.11
Bacteria; Chlamydiae	0.00	0.00	0.15	0.00	0.00	0.00
Bacteria; Tenericutes	0.00	0.00	0.00	0.00	0.00	1.99
Bacteria; Elusimicrobia	0.00	0.00	0.13	0.00	0.00	0.00

1006 First, exogenous microbial DNA from the environment has been shown to
1007 dominate porous ancient samples, such as bone. In addition, bacterial DNA can be
1008 regularly isolated from laboratory reagents[34], likely overpowering the initial signal
1009 from endogenous oral microorganisms. To assess the impacts of exogenous DNA on
1010 these differences, data sets with the environmental and laboratory microorganisms
1011 removed were compared to unfiltered data (Figure 1). While this did not correct the
1012 differences between the shotgun and amplicon sequencing approaches (Extended Data
1013 Figure 1), it did enhance the endogenous signal from the historic specimen
1014 (chimpanzee) and one ancient sample (El Sidrón 2) (Figure 1). To accurately assess
1015 ancient data sets, the levels and contributions of contaminant DNA need to be
1016 included.

1017 Second, the damage and fragmentation of ancient DNA is also likely to limit
1018 species detection and identification in amplicon libraries. 16S rRNA reads in ancient
1019 metagenomes averaged 74.7 bp (Table S6) – well below the size required for robust
1020 taxa identification (100 bp) or detection with gold-standard 16S primer sets (269
1021 bp)[88]. However, larger 16S sequences (up to 181 bp) were identified in the shotgun
1022 data set, and their community structure was comparable to the profile from the whole
1023 shotgun data set (Figure 1), suggesting that shorter 16S rRNA amplicon fragments or
1024 hybridization enrichment may provide more accurate pictures of ancient community
1025 diversity. In addition, UPGMA clustering filtered 16S rRNA amplicon libraries with
1026 25 additional amplicon libraries generated from samples by Adler *et al*[1] (n=49) (Table
1027 S1) was able to resolve some differences between ancient samples (ancient
1028 agriculturalists from hunter-gatherers; ancient agriculturalists from modern humans;
1029 Extended Data Figure 2), suggesting that some longer single stranded 16S rRNA

fragments are stable in dental calculus and that increased sample size of amplicon data may provide useful information in some cases, likely with less ancient material.

Earlier studies have hypothesized that taphonomic biases of ancient bacterial communities may occur different in select phyla, *i.e.* those with weaker outer cell wall structures compared to those with robust peptidoglycan matrices[1] or in specific taxa with smaller 16S rRNA sizes in specific regions (V3)[90]. To determine if differences between 16S amplicon and shotgun data sets were limited to select phyla, filtered and unfiltered data sets were directly compared (Extended Data Figure 1). Each ancient sample had biases in certain phyla, although only biases in archaeal phyla appear to be shared across multiple ancient specimens (Table S16), which is likely a result of bias introduced during 16S amplicon library construction using conserved bacterial primer sets[90]. Overall, Gram-positive and Gram-negative phyla were equally impacted, and no particular phyla appeared to be systemically biased in all ancient specimens. Together, these observations highlight significant issues with solely utilizing 16S rRNA amplification for the analysis of ancient metagenomes and indicate that further sequencing of larger data sets is necessary to understand the taphonomic processes at work on ancient bacterial communities.

References

1. Adler, C. J. *et al.* Sequencing ancient calcified dental plaque shows changes in oral microbiota with dietary shifts of the Neolithic and Industrial revolutions. *Nat. Genet.* **45,** 450–455 (2013).
2. Price, T. D. *et al.* in *Fundberichte aus Baden-Württemberg* (ed. Funda, D. T.) 23–58 (Kommissionsverlag Konrad Theiss Verlag, 2003).
3. Semal, P. *et al.* New data on the late Neandertals: Direct dating of the Belgian Spy fossils. *Am. J. Phys. Anthropol.* **138,** 421–428 (2009).
4. Lalueza-Fox, C. *et al.* Genetic evidence for patrilocal mating behavior among Neandertal groups. *Proc. Natl. Acad. Sci.* **108,** 250–253 (2011).
5. Dean, M. C. *et al.* Longstanding dental pathology in Neandertals from El Sidrón (Asturias, Spain) with a probable familial basis. *J. Hum. Evol.* **64,** 678–686 (2013).
6. Manzi, G. & Passarello, P. At the Archaic/Modern Boundary of the Genus Homo: The Neandertals From Grotta Breuil. *Curr. Anthropol.* **36,** 355–366 (1995).
7. Buckley, S., Usai, D., Jakob, T., Radini, A. & Hardy, K. Dental Calculus Reveals Unique Insights into Food Items, Cooking and Plant Processing in Prehistoric Central Sudan. *PLoS ONE* **9,** e100808 (2014).
8. Arkell, A. J. *Shaheinab, an Account of the Excavation of a Neolithic Occupation Site Carried Out for the Sudan Antiquities Service in 1949-50, by A. J. Arkell,...* (Oxford University Press, 1953).
9. The Lech Krzyzaniak Excavations in the Sudan, Kadero, Studies in Afric. Available at: http://www.archeobooks.com/products/the-lech-krzyzaniak-excavations-in-the-sudan-kadero-studies-in-african-archaeology-vol-10. (Accessed: 9th October 2015)

10. Madella, M., García-Granero, J. J., Out, W. A., Ryan, P. & Usai, D. Microbotanical Evidence of Domestic Cereals in Africa 7000 Years Ago. *PLoS ONE* **9,** e110177 (2014).
11. Morris, A. G. *A Master Catalogue: Holocene Human Skeletons from South Africa*. (Witwatersrand Univ Pr, 1993).
12. Mitchell, P. *The Archaeology of Southern Africa*. (Cambridge University Press, 2002).
13. Mountain, A. *The First People of the Cape: A Look at Their History and the Impact of Colonialism on the Cape's Indigenous People*. (New Africa Books, 2003).
14. Sealy, J. C., Patrick, M. K., Morris, A. G. & Alder, D. Diet and dental caries among later stone age inhabitants of the Cape Province, South Africa. *Am. J. Phys. Anthropol.* **88,** 123–134 (1992).
15. Reenen, J. F. V. Dental Features of a Low-Caries Primitive Population. *J. Dent. Res.* **45,** 703–713 (1966).
16. Morris, A. G. *et al.* Later Stone Age burials from the Western Cape Province, South Africa Part 1: Voelvlei. *South. Afr. Field Archaeol.* **13 & 14,** 19–26
17. Cronin, M. Radiocarbon dates for the Early Iron Age in Transkei. *South Afr. J. Sci.* **78,** 38–39 (1982).
18. Morris, A. *The Skeletons of Contact: Protohistoric burials from the lower Orange River Valley*. (Johannesburg: Witwatersrand University Press, 1992).
19. Wiegelmann, H. j T. and G. *Der Wandel der Nahrungsgewohnheiten unter dem Einfluß der Industrialisierung. (Studien zum Wandel von Gesellschaft und Bildung im 19. Jahrhundert)*. (Göttingen: Vandenhoek & Ruprecht).

20. Brotherton P, Haak W, Templeton J, Brandt G, Soubrier J, Adler CJ, Richards SM, Der Sarkissian C, Ganslmeier R, Friederich S, Dresely V, van Oven M, Kenyon R, Van der Hoek M, Korlach J, Luong K, Ho SYW, Quintana-Murci L, Behar DM, Meller H, Alt KW, Cooper A & The Genographic Project. Neolithic mitochondrial haplogroup H genomes and the genetic origins of Europeans. *Nat. Commun.* **4**:1764.

21. Caporaso, J. G. *et al.* Ultra-high-throughput microbial community analysis on the Illumina HiSeq and MiSeq platforms. *ISME J.* **6,** 1621–1624 (2012).

22. Cooper, A. & Poinar, H. N. Ancient DNA: Do It Right or Not at All. *Science* **289,** 1139–1139 (2000).

23. Acinas, S. G., Sarma-Rupavtarm, R., Klepac-Ceraj, V. & Polz, M. F. PCR-Induced Sequence Artifacts and Bias: Insights from Comparison of Two 16S rRNA Clone Libraries Constructed from the Same Sample. *Appl. Environ. Microbiol.* **71,** 8966–8969 (2005).

24. Gonzalez, J. M., Portillo, M. C., Belda-Ferre, P. & Mira, A. Amplification by PCR Artificially Reduces the Proportion of the Rare Biosphere in Microbial Communities. *PLoS ONE* **7,** e29973 (2012).

25. Aronesty, E. *Command-line tools for processing biological sequencing data*. (2011).

26. Martin, M. Cutadapt removes adapter sequences from high-throughput sequencing reads. *EMBnet.journal* **17,** 10–12 (2011).

27. Caporaso, J. G. *et al.* QIIME allows analysis of high-throughput community sequencing data. 335–336 (2010).

28. Edgar, R. C. Search and clustering orders of magnitude faster than BLAST. 2460–2461 (2010).

29. DeSantis, T. Z. *et al.* Greengenes, a Chimera-Checked 16S rRNA Gene Database and Workbench Compatible with ARB. *Appl. Environ. Microbiol.* **72,** 5069–5072 (2006).

30. Wang, Q., Garrity, G. M., Tiedje, J. M. & Cole, J. R. Na?ve Bayesian Classifier for Rapid Assignment of rRNA Sequences into the New Bacterial Taxonomy. *Appl. Environ. Microbiol.* **73,** 5261–5267 (2007).

31. Warinner, C. *et al.* Pathogens and host immunity in the ancient human oral cavity. *Nat Genet* **46,** 336–344 (2014).

32. Rougier, H. *Spy Cave: 125 Years of Multidisciplinary Research at the Betche Aux Rotches (Jemeppe-sur-Sambre, Province of Namur, Belgium)*. (Société Royale Belge d'Anthropologie et de Préhistoire, 2012).

33. Hofreiter, M., Serre, D., Poinar, H. N., Kuch, M. & Pääbo, S. Ancient DNA. *Nat. Rev. Genet.* **2,** 353–359 (2001).

34. Salter, S. J. *et al.* Reagent and laboratory contamination can critically impact sequence-based microbiome analyses. *BMC Biol.* **12,** (2014).

35. Schmieder, R. & Edwards, R. Fast Identification and Removal of Sequence Contamination from Genomic and Metagenomic Datasets. *PLoS ONE* **6,** e17288 (2011).

36. Ramirez, K. S., Lauber, C. L. & Fierer, N. Microbial consumption and production of volatile organic compounds at the soil-litter interface. *Biogeochemistry* **99,** 97–107 (2010).

37. Adler, C. J. *et al.* Sequencing ancient calcified dental plaque shows changes in oral microbiota with dietary shifts of the Neolithic and Industrial revolutions. *Nat. Genet.* (2013). doi:10.1038/ng.2536

38. Chen, T. *et al.* The Human Oral Microbiome Database: a web accessible resource for investigating oral microbe taxonomic and genomic information. *Database J. Biol. Databases Curation* **2010,** baq013 (2010).

39. Meyer, M. & Kircher, M. Illumina sequencing library preparation for highly multiplexed target capture and sequencing. *Cold Spring Harb. Protoc.* **2010,** pdb prot5448 (2010).

40. Herbig, A. *et al.* MALT: Fast alignment and analysis of metagenomic DNA sequence data applied to the Tyrolean Iceman. *bioRxiv* 50559 (2016). doi:10.1101/050559

41. Buchfink, B., Xie, C. & Huson, D. H. Fast and sensitive protein alignment using DIAMOND. *Nat Meth* **12,** 59–60 (2015).

42. Huson, D. H., Mitra, S., Ruscheweyh, H.-J., Weber, N. & Schuster, S. C. Integrative analysis of environmental sequences using MEGAN4. 1552–1560 (2011).

43. Huson, D. H. SplitsTree: analyzing and visualizing evolutionary data. *Bioinforma. Oxf. Engl.* **14,** 68–73 (1998).

44. Segata, N. *et al.* Metagenomic biomarker discovery and explanation. *Genome Biol.* **12,** R60 (2011).

45. Li, H. & Durbin, R. Fast and accurate short read alignment with Burrows-Wheeler transform. *Bioinformatics* **25,** 1754–1760 (2009).

46. Schubert, M. *et al.* Improving ancient DNA read mapping against modern reference genomes. *BMC Genomics* **13,** 178 (2012).

47. Kircher, M. Analysis of high-throughput ancient DNA sequencing data. *Methods Mol. Biol.* **840,** 197–228 (2012).

48. Ginolhac, A., Rasmussen, M., Gilbert, M. T., Willerslev, E. & Orlando, L. mapDamage: testing for damage patterns in ancient DNA sequences. *Bioinformatics* **27,** 2153–5 (2011).

49. Kearse, M. *et al.* Geneious Basic: An integrated and extendable desktop software platform for the organization and analysis of sequence data. 1647–1649 (2012).

50. Krzywinski, M. I. *et al.* Circos: An information aesthetic for comparative genomics. *Genome Res.* (2009). doi:10.1101/gr.092759.109

51. Darling, A. E., Mau, B. & Perna, N. T. progressiveMauve: Multiple Genome Alignment with Gene Gain, Loss and Rearrangement. *PLoS ONE* **5,** e11147 (2010).

52. Talavera, G. & Castresana, J. Improvement of Phylogenies after Removing Divergent and Ambiguously Aligned Blocks from Protein Sequence Alignments. *Syst. Biol.* **56,** 564–577 (2007).

53. Stamatakis, A. RAxML-VI-HPC: maximum likelihood-based phylogenetic analyses with thousands of taxa and mixed models. 2688–2690 (2006).

54. Stamatakis, A. RAxML-VI-HPC: maximum likelihood-based phylogenetic analyses with thousands of taxa and mixed models. *Bioinformatics* **22,** 2688–90 (2006).

55. Drummond, A. J. & Rambaut, A. BEAST: Bayesian evolutionary analysis by sampling trees. *BMC Evol. Biol.* **7,** 214 (2007).

56. Cock, P. J. A. *et al.* Biopython: freely available Python tools for computational molecular biology and bioinformatics. *Bioinformatics* **25,** 1422–1423 (2009).

57. Longo, M. S., O'Neill, M. J. & O'Neill, R. J. Abundant Human DNA Contamination Identified in Non-Primate Genome Databases. *PLOS ONE* **6,** e16410 (2011).

58. Mukherjee, S., Huntemann, M., Ivanova, N., Kyrpides, N. C. & Pati, A. Large-scale contamination of microbial isolate genomes by Illumina PhiX control. *Stand. Genomic Sci.* **10,** 18 (2015).

59. Knights, D. *et al.* Bayesian community-wide culture-independent microbial source tracking. *Nat. Methods* **8,** 761–763 (2011).

60. Hewitt, K. M. *et al.* Bacterial Diversity in Two Neonatal Intensive Care Units (NICUs). *PLoS ONE* **8,** e54703 (2013).

61. Allentoft, M. E. *et al.* The half-life of DNA in bone: measuring decay kinetics in 158 dated fossils. *Proc. R. Soc. B Biol. Sci.* rspb20121745 (2012). doi:10.1098/rspb.2012.1745

62. R Development Core Team. *R: A language and envrionment for statistical computing, reference index version 2.x.x.* (R Foundation for Statistical Computing).

63. Martiny, J. B. H. *et al.* Microbial biogeography: putting microorganisms on the map. *Nat. Rev. Microbiol.* **4,** 102–112 (2006).

64. Bollongino, R. *et al.* 2000 Years of Parallel Societies in Stone Age Central Europe. *Science* **342,** 479–481 (2013).

65. Gumiński, W. *The peat-bog site Dudka, Masurian Lakeland: an example of conservative economy.* (Sheffield Academic Press, 1998).

66. Poinar, H. N. *et al.* Metagenomics to paleogenomics: large-scale sequencing of mammoth DNA. *Science* **311,** 392–394 (2006).

67. Frampton, M. & Houlston, R. Generation of Artificial FASTQ Files to Evaluate the Performance of Next-Generation Sequencing Pipelines. *PLoS ONE* **7,** e49110 (2012).

68. Meyer, F. *et al.* The metagenomics RAST server – a public resource for the automatic phylogenetic and functional analysis of metagenomes. 386 (2008).

69. Segata, N. *et al.* Metagenomic microbial community profiling using unique clade-specific marker genes. *Nat. Methods* **9,** 811–814 (2012).

70. Lindgreen, S., Adair, K. L. & Gardner, P. P. An evaluation of the accuracy and speed of metagenome analysis tools. *Sci. Rep.* **6,** 19233 (2016).

71. Belda-Ferre, P. *et al.* The oral metagenome in health and disease. *ISME J.* **6,** 46–56 (2012).

72. Lazarevic, V. *et al.* Metagenomic study of the oral microbiota by Illumina high-throughput sequencing. *J. Microbiol. Methods* **79,** 266–271 (2009).

73. Cameron, S. J. S., Huws, S. A., Hegarty, M. J., Smith, D. P. M. & Mur, L. A. J. The human salivary microbiome exhibits temporal stability in bacterial diversity. *FEMS Microbiol. Ecol.* **91,** fiv091 (2015).

74. Moeller, A. H. *et al.* Rapid changes in the gut microbiome during human evolution. *Proc. Natl. Acad. Sci.* **111,** 16431–16435 (2014).

75. Haak, W. *et al.* Massive migration from the steppe was a source for Indo-European languages in Europe. *Nature* **522,** 207–211 (2015).

76. Briggs, A. W. *et al.* Targeted Retrieval and Analysis of Five Neandertal mtDNA Genomes. *Science* **325,** 318–321 (2009).

77. Schuenemann, V. J. *et al.* Genome-Wide Comparison of Medieval and Modern Mycobacterium leprae. *Science* **341,** 179–183 (2013).

78. Ozga, A. T. *et al.* Successful enrichment and recovery of whole mitochondrial genomes from ancient human dental calculus. *Am. J. Phys. Anthropol.* **160,** 220–228 (2016).

79. Brockmeier, S. L. & Register, K. B. Expression of the dermonecrotic toxin by Bordetella bronchiseptica is not necessary for predisposing to infection with toxigenic Pasteurella multocida. *Vet Microbiol* **125,** 284–9 (2007).

80. Parkhill, J. *et al.* Comparative analysis of the genome sequences of Bordetella pertussis, Bordetella parapertussis and Bordetella bronchiseptica. *Nat Genet* **35,** 32–40 (2003).

81. Scarre, C. *The Human Past: World Prehistory and the Development of Human Societies*. (Thames & Hudson, 2013).

82. Bocquet-Appel, J.-P. & Bar-Yosef, O. *The Neolithic Demographic Transition and its Consequences*. (Springer Science & Business Media, 2008).

83. van der Zee, A., Mooi, F., Van Embden, J. & Musser, J. Molecular evolution and host adaptation of Bordetella spp.: phylogenetic analysis using multilocus enzyme electrophoresis and typing with three insertion sequences. *J. Bacteriol.* **179,** 6609–6617 (1997).

84. Bos, K. I. *et al.* A draft genome of Yersinia pestis from victims of the Black Death. 506–510 (2011).

85. Duchêne, S., Geoghegan, J. L., Holmes, E. C. & Ho, S. Y. Estimating evolutionary rates using time-structured data: a general comparison of phylogenetic methods. *Bioinformatics* btw421 (2016). doi:10.1093/bioinformatics/btw421

86. Stringer, C. The origin and evolution of Homo sapiens. *Phil Trans R Soc B* **371,** 20150237 (2016).

87. Sharpton, T. J. An introduction to the analysis of shotgun metagenomic data. *Front. Plant Sci.* **5,** (2014).

88. Liu, Z., Lozupone, C., Hamady, M., Bushman, F. D. & Knight, R. Short pyrosequencing reads suffice for accurate microbial community analysis. *Nucleic Acids Res.* **35,** e120 (2007).

89. Lozupone, C. & Knight, R. UniFrac: a New Phylogenetic Method for Comparing Microbial Communities. 8228–8235 (2005).

90. Ziesemer, K. A. *et al.* Intrinsic challenges in ancient microbiome reconstruction using 16S rRNA gene amplification. *Sci. Rep.* **5,** 16498 (2015).